AD-A085 514 MONTANA STATE UNIV BOZEMAN SUPERSONIC WIND TUNNEL LAB F/G 20/4
NECESSARY CONDITIONS FOR TRANSITION IN A FREE SHEAR LAYER.(U)
FEB 80 A DEMETRIADES F49620-79-C-0210
UNCLASSIFIED SWT-80-1 AFOSR-TR-80-0442 NL

1 OF 1
AD
A085514

END
DATE
FILMED
7-80
DTIC

SECURITY CLASSIFICATION OF THIS PAGE (When Data Entered)

REPORT DOCUMENTATION PAGE		READ INSTRUCTIONS BEFORE COMPLETING FORM
1. REPORT NUMBER AFOSR-TR-80-0442	2. GOVT ACCESSION NO. AD-A085514	3. RECIPIENT'S CATALOG NUMBER
4. TITLE (and Subtitle) NECESSARY CONDITIONS FOR TRANSITION IN A FREE SHEAR LAYER		5. TYPE OF REPORT & PERIOD COVERED AFOSR SCIENTIFIC REPORT 1 Aug. 79 - 31 Jan. 80
		6. PERFORMING ORG. REPORT NUMBER SWT Report No. 80-1
7. AUTHOR(s) Anthony Demetriades		8. CONTRACT OR GRANT NUMBER(s) F49620-79-C-0210
9. PERFORMING ORGANIZATION NAME AND ADDRESS Mechanical Engineering Department Montana State University Bozeman, Montana 59717		10. PROGRAM ELEMENT, PROJECT, TASK AREA & WORK UNIT NUMBERS 2307/A2 61102F
11. CONTROLLING OFFICE NAME AND ADDRESS AIR FORCE OFFICE OF SCIENTIFIC RESEARCH/NA BUILDING 410 BOLLING AFB, DC 20332		12. REPORT DATE February 1980
		13. NUMBER OF PAGES 52
14. MONITORING AGENCY NAME & ADDRESS (if different from Controlling Office)		15. SECURITY CLASS. (of this report) Unclassified
		15a. DECLASSIFICATION DOWNGRADING SCHEDULE

16. DISTRIBUTION STATEMENT (of this Report)

Approved for public release; distribution unlimited.

17. DISTRIBUTION STATEMENT (of the abstract entered in Block 20, if different from Report)

18. SUPPLEMENTARY NOTES

19. KEY WORDS (Continue on reverse side if necessary and identify by block number)

Supersonic, shear layer, transition, turbulence

20. ABSTRACT (Continue on reverse side if necessary and identify by block number)

A necessary condition for the preservation of turbulence has been utilized to predict laminar-turbulent transition in free shear, or mixing, layers. Following earlier applications in wakes and boundary layers, the condition is expressed in terms of a threshold turbulence Reynolds number which can be computed if the turbulence properties of the post-transitional flow are known. Assuming that the latter are those reported for self-similar flows, general rules for transition in all major types of shear flows are drawn. Numerical computations are presented for arbitrary homogeneous free shear layer transition >over

DD FORM 1 JAN 73 1473

411798

SECURITY CLASSIFICATION OF THIS PAGE (When Data Entered) identified as the most forward permissible turbulence onset location. Transition is found to move downstream very rapidly as the fast-stream Mach number is increased and the speed ratio is decreased, and less rapidly as the slow stream is heated. Agreement with available transition data is qualitatively good but quantitatively fair, which is ascribed to missing information about the shear layer turbulence and the observed tendency of available transition data to depend on the Reynolds number.

TABLE OF CONTENTS

PREFACE

This report describes work performed in the Mechanical Engineering Department of Montana State University under USAFOSR Contract No. F49620-79-5-0210 and addresses the problem of laminar-turbulent transition in a homogeneous free-shear, or "mixing" layer. The work extends recent research performed by its author while in another organization, in applying a novel first-principles approach to transition in parallel shear flows. Cited references herein describe previous applications of the same principle to boundary layers and wakes.

The encouragement of Lieutenant Colonel L. Ormand of AFOSR toward the present program is gratefully acknowledged. Helpful technical comments in this research were frequently received from P. J. Ortwerth of AFWL. Thanks are also due A. J. Laderman and W. Moeny; to the former for contributions regarding the Crocco relation, and to the latter for providing approximate self-similar forms of the laminar shear layer growth.

ABSTRACT

A necessary condition for the preservation of turbulence has been utilized to predict laminar-turbulent transition in free shear, or mixing, layers. Following earlier applications in wakes and boundary layers, the condition is expressed in terms of a threshold turbulence Reynolds number which can be computed if the turbulence properties of the post-transitional flow are known. Assuming that the latter are those reported for self-similar flows, general rules for transition in all major types of shear flows are drawn. Numerical computations are presented for arbitrary homogeneous free shear layer transition, identified as the most forward permissible turbulence onset location. Transition is found to move downstream very rapidly as the fast-stream Mach number is increased and the speed ratio is decreased, and less rapidly as the slow stream is heated. Agreement with available transition data is qualitatively good but quantitatively fair, which is ascribed to missing information about the shear layer turbulence and the observed tendency of available transition data to depend on the unit Reynolds number.

LIST OF SYMBOLS

b	flow width
C	constant in the transition equation (virtual origin reference)
C'	constant in the transition equation (thickness reference)
C''	$= C'^2$
c_1	proportion of integral scale to flow thickness
DSL	dividing streamline
FSL	free shear layer
$g(M_1)$	growth function of FSL thickness
G	nondimensional laminar FSL thickness
h	FSL thickness
k	exponent of the temperature-viscosity relation
K	nondimensional variable (reference: laminar thickness)
L	transverse scale of turbulent flow
M	Mach number
n	exponent in generalized flow width formulas
P	pressure
R_1	nondimensional velocity ratio = u_2/u_1
R_3	nondimensional total temperature ratio = T_{o2}/T_{o1}
Re_Λ	turbulence Reynolds number
$Re_{\Lambda o}$	threshold value of Re_Λ
Re_λ	Reynolds number based on dissipation scale
Re_T	turbulent Reynolds number

Re_b	Reynolds number based on constant length
Re_{xo}	transition Reynolds number based on x_{oT}
Re_{1x}	Reynolds number based on fast-side properties and x
Re_{hT}	transition Reynolds number based on thickness
Re_{xT}	transition Reynolds number based on distance from the flow origin
T	temperature
T_o	stagnation temperature
u	velocity
u^*	DSL velocity
w	velocity defect
x	distance along flow
x_o	distance from flow origin to the virtual turbulence origin
x_{oT}	distance from virtual origin to transition
γ	specific heat ratio
$\Gamma(M_1)$	nondimensional velocity fluctuation magnitude
δ	shear layer thickness (laminar)
Δu	velocity difference (maximum) across flow
ϵ	dissipation
η	nondimensional lateral coordinate
λ	nondimensional velocity ratio $(u_1-u_2)/(u_1 + u_2)$; dissipation scale (the latter in Section 3 only)
Λ	integral scale (macroscale)
ν	kinematic viscosity
ν_t	turbulent kinematic viscosity
ξ	distance from virtual origin

σ_o	FSL incompressible spreading parameter
$(\ )_1$	fast-side properties
$(\ )_2$	slow-side properties
$(\ )_{DSL}$	properties along the DSL
$(\ )'$	turbulent component
$(\ )(0)$	quantity in center of flow
$(\ )_e$	quantity at flow edge
$(\ )_t$	turbulent quantity
$(\ )_l$	laminar quantity
$(\ )_T$	at transition (except ν_T)

FIGURE CAPTIONS

1. Movement of the "transition point" x_T when the flow Reynolds number Re_b increases, for flows with turbulence Reynolds numbers increasing in the downstream direction.

2. Flow-field definition

3. Transition Reynolds number based on the distance from the virtual origin of turbulence (adiabatic case).

4. Transition Reynolds number based on the distance from the virtual origin of turbulence, with and without heat transfer.

5. Transition Reynold number based on the FSL thickness at transition, for the adiabatic and heated cases.

6. Details of the transition Reynolds number based on the FSL thickness, for the cooled case.

7. Transition Reynolds number based on thickness, for the case where one side of the FSL is at zero velocity, showing the effect of heat transfer.

8. Laminar FSL thickness, primarily for the adiabatic and heated cases; the incompressible behavior is shown in the inset.

9. Laminar FSL thickness for the cooled case.

10. Transition Reynolds number based on distance from the actual flow origin: adiabatic and heated cases

11. Transition Reynolds number based on distance from the actual flow origin: cooled case

12. Transition Reynolds number cross-plotted for the case $\lambda = 1$ to show effect of heat transfer

13. Relative position of the virtual origin of turbulence in a shear layer: adiabatic and heated cases.

14. Relative position of the virtual origin of turbulence in a shear layer: cooled case

15. Comparison of the present theory with experimental results, for the homogeneous adiabatic case (air)

16. Comparison of the present theory with experimental results, for the homogeneous adiabatic case (air)

17. Minimum permitted stagnation temperature for FSL flows if M_1 and λ are specified

18. Dividing streamline temperatures

1. INTRODUCTION AND BACKGROUND

It is a telling point in the attempts to predict theoretically the onset of laminar-turbulent transition, that progress in that direction in the past half century has roughly paralleled progress in understanding the turbulence itself.

The change of a physical system from one state to another can be understood only to the extent to which each state is separately understood. The transition process will therefore remain obscure as long as turbulence itself remains obscure. It is, conversely, not too drastic a statement to make that the theory which first provides a mathematical description of the complete transition process will also be first in supplying the tools for describing the turbulent state.

The present study had its inception some years ago when the author was engaged with experimental research in the hydrodynamic stability of boundary layers, while also pursuing a combined experimental-theoretical compendium of wake flows. Transition to turbulence was a feature of both of these studies, and the author's plan was to seek an independent necessary condition, or threshold, for the establishment of turbulence much as a minimum critical Reynolds number exists for the establishment of hydrodynamic instability.

The first attempt to find and apply such a necessary condition dealt with wake flows, and resulted in an algebraic expression for a Reynolds number based on a physical length connecting the flow origin with a region in the flow beyond which conditions were proper for the establishment of self-preserving turbulence. Surprisingly, this Reynolds number also agreed qualitatively and quantitatively with transition Reynolds numbers observed for wakes. This agreement justified the risk of associating the necessary condition with the transition phenomenon, and it was so proposed in the journal publication which followed [1].

The apparent success of the necessary threshold also justified, at this time, its extension to other flows. The application to boundary layers followed in 1978, and the results were published in references 2 and 3. Considering the scarcity of inputs needed to make detailed computations, the boundary layer threshold results also gave more than satisfactory agreement with boundary layer transition data. The dependence of the transition (momentum) Reynolds number on Mach number and temperature ratio were in good qualitative agreement with the results, and phenomena such as transition reversal were rationalized. Again because of this similarity, the results of applying the necessary condition were continued to be discussed as laminar-turbulent transition predictions.

The present report presents the application of the necessary condition ("threshold" or "dissipation" theory) to a yet third type of parallel shear flow which is the free shear layer (FSL) also called the "mixing layer." The motivation for this work stemmed from problems in gas-dynamic and chemical laser applications. Once more the application of the threshold motion is represented as an attempt to predict transition.

The approach hinges on exploiting the indisputable requirement that turbulence cannot preserve itself unless the viscous dissipation decreases below a certain level relative to the turbulence inertia. The only new elements involved are the assignment of a specific numerical value to this threshold in the form of a minimum turbulence Reynolds number, the computation of this number for the flow in question, and the assumption that the wetted length (or momentum thickness) resulting from this computation represents a sufficient, as well as a necessary, quantity in describing the turbulence onset. These elements were first discussed in reference 4, and an improved discussion in some detail is repeated in Section 4 of this report.

In the same section, all typical parallel flows are discussed in the light of the turbulence Reynolds number, and some implications about transition in each are drawn. The application to the free-shear-layer transition problem is then presented in Section 5.

2. OUTLINE OF THE METHOD

The transition estimation method followed in References 1, 2, 3, and 4, and the present report is as follows. The flow whose transition characteristics are desired is first assumed fully turbulent and its turbulence Reynolds number

$$Re_\Lambda \equiv \frac{u'\Lambda}{\nu} \qquad (1)$$

is computed using the available knowledge of u', Λ and ν. This calculation reveals certain regions of the flow (e.g. upstream of a certain point) where Re_Λ lies below some previously determined threshold value $Re_{\Lambda o}$. This "point" is taken to be the location of laminar-turbulent transition. To be successful in this approach we need to (a) agree on the general principle of turbulence quenching by viscosity, (b) determine an approximate value for $Re_{\Lambda o}$, (c) translate the criterion into an algebraic expression for a transition Reynolds number and (d) demonstrate that the necessary condition is also sufficient.

That viscosity can effectively quench turbulence is assumed as agreed upon; the subject is hardly controversial, and is discussed in a number of texts (e.g. References 5 and 6). On the other end of the scale, sufficiency cannot be demonstrated; this approach can at present only rest its case "a posteriori" on the strength of usually good qualitative and adequate numerical agreement with transition data, and on benefits such as the emergence of the algebraic dependence of transition on the relevant variables. An attempt to qualify the approach and to state its limitations will be given in Section 5.

In the following discussion we will present justification for the choice of the threshold functional and of the approximate value chosen for it; and in Section 5 we will demonstrate its use in the free-shear-layer problem.

3. DETERMINATION OF THE THRESHOLD REYNOLDS NUMBER

It is frequently mentioned that a proper measure of the effect of viscous forces on turbulence is the turbulence Reynolds number defined by Equation (1). In an order-of-magnitude sense, quenching of turbulence occurs "when Re_{Λ} is of order or smaller than unity." This author sought to quantify this phrase by invoking experimental evidence, as discussed in References 1 and 2. From experiments in decaying isotropic turbulence reported in the literature, [7], [8], and [9], it was concluded that $Re_{\Lambda o}$ lay between about 10 and 20. Also, by inverting the present procedure (i.e. by invoking transition data to compute $Re_{\Lambda o}$) Reference 1, Figure 2, demonstrates that an approximate value of 15 will serve.

An interesting method of obtaining another estimate of the threshold $Re_{\Lambda o}$ is obtained if we consider the effect of *decreasing Reynolds number* on the turbulence spectrum. Of the many characteristic lengths (or wavenumbers, or frequencies) important to the behavior of the spectrum, consider the integral scale Λ and the dissipation scale λ. In physical terms Λ represents the largest division (or "eddy size") of the turbulence, typically within an order of magnitude smaller than the lateral flow dimension (e.g. the shear layer thickness) and so fixed by the latter independently of Reynolds number. It is implicit in the present approach that turbulence cannot exist in the particular flow discussed if this scale is caused, by viscosity, to exist in sizes much larger than stated above. As seen in Section 5.2, this scale is taken to be a fixed fraction of the lateral flow dimension.

The dissipation microscale λ, however, is a measure of the smallest eddies allowed to develop by viscosity, and is thus controlled by the flow Reynolds number. As the Reynolds number decreases, λ increases; but since $\lambda < \Lambda$ by definition, this increase means that λ approaches Λ. This results in a depopulation of the spectrum energy at its higher wavenumbers while the lower end of the spectrum remains unchanged, as demonstrated by Uberoi and his coworkers [10]. Obviously, λ cannot forever keep increasing as the Reynolds number decreases, and its maximum value must be Λ; any decrease of the Reynolds number beyond that point will eradicate the turbulence itself, as mentioned above.

Hinze formulates some interesting connections between λ and Λ in his discussion of isotropic turbulence [6, eqs. 3-106ff]. By equating the viscous dissipation rate

$$\varepsilon = 15\nu \frac{u'^2}{\lambda^2} \tag{2}$$

with the power supplied per unit mass to the smaller eddies,

$$\varepsilon = A \frac{u'^3}{\Lambda} \tag{3}$$

he obtains the following relation between the Reynolds numbers formed with Λ and λ respectively:

$$Re_\Lambda = \frac{A}{15} Re_\lambda 2 \tag{4}$$

Since, according to Hinze, A is of "order unity," it follows from Equation (4) that the minimum condition for the existence of turbulence $\lambda = \Lambda$ (i.e. $Re_\lambda = Re_\Lambda$) would give

$$Re_{\Lambda o} \simeq 15 \tag{5}$$

which agrees with our choice as mentioned above.

(The identification of the proportionality constant A with unity is not explained by Hinze, however. Equation (5) is at best an approximation, although the numerical "agreement" with our criterion certainly deserves the present mention. Hinze's discussion on the effect of characteristic length scales on isotropic turbulence (Chapter 3 of Reference 6) is in any way important in our present context).

Another method of arriving at the dissipation criterion is offered by Ortwerth [11] who equated the laminar and turbulent dissipation at the point of maximum shear of the flow. This criterion is expressed as

$$\frac{u' l_e}{\nu} = 36 \tag{6}$$

where l_e is the FSL width defined by the tangent at the maximum shear region and is related to the actual width h by $l_e \simeq 0.5h$. Using $h = 5\Lambda$ as was done in Reference 1, we find that Equation (6) becomes

$$\frac{u'\Lambda}{\nu} = Re_{\Lambda o} = 14.4 \tag{7}$$

Here is, therefore, a different approach to the necessary condition which is in close numerical agreement to our threshold of Equation (5).

Historically, Townsend [5] was among the first to recognize that the threshold between the laminar and turbulent states can be predicted, at least qualitatively, by a comparison of the eddy viscosity with the molecular viscosity. In discussing the apparent constancy of a "turbulent" Reynolds number

$$Re_T = \frac{L\Delta u}{\nu_T} = \text{const.} \tag{8}$$

for wake flows in general, he notes the peculiar properties of axisymmetric turbulent wakes which he calls the "final period." In such wakes, the transverse scale L of the flow increases as the 1/3 power of distance, while the velocity decrement Δu decreases as the -2/3 power of distance. The numerator of Equation (8) thus decreases as the -1/3 power of distance, and to keep the ratio constant, the eddy viscosity ν_T should follow suit. In axisymmetric wakes, therefore, the eddy kinematic viscosity will ultimately fall (far downstream) below the magnitude of the molecular viscosity and turbulence will be "quenched." This situation is unique to the axisymmetric wake only, as also recognized in our own present framework of the turbulence Reynolds number Re_Λ (see Section 4). It is interesting that Townsend's discussion pertains to relaminarization rather than transition, portending the capability of the present approach to address this phenomenon as well.

It is also pertine t that Lees [12] extended Townsend's concepts in this regard, deriving e. timates for the minimum Reynolds number capable of generating turbulence in two-dimensional wakes. This provided background for this author's more ambitious undertaking of wake transition predictions [1] by assuming that the necessary condition is also sufficient.

Arguments such as those presented above seem to show that, for purposes of making numerical estimates of transition location, a value of $Re_{\Lambda o} = 15$ is an acceptable first approximation. However, the issue is far from settled, and the question whether $Re_{\Lambda o}$ is "universal" remains open. In the meantime, the value of $Re_{\Lambda o} = 15$ will be used for FSL transition calculations in Section 5, since the universality argument would be strengthened by proof of "successful" predictions for all flows using a single $Re_{\Lambda o}$ value. In fact, in the FSL computations of Section 5, the $Re_{\Lambda o}$ will be combined with other "universal" constants (such as the incompressible spreading parameter σ_o) into a constant C; numerical inadequacies of the present method could then be attributed to lack of data about such critical numbers, encouraging research into their precise determination.

4. THE TURBULENCE REYNOLDS NUMBER IN PARALLEL SHEAR FLOWS

The present approach to the FSL transition question revolves around the magnitude of the turbulence Reynolds number

$$Re_\Lambda \equiv \frac{\Lambda u'}{\nu} \tag{1}$$

in the shear layer. However, the approach is equally relevant to all parallel shear flows. A brief general discussion of the behavior of Re_Λ in representative examples of such flows will be therefore given below.

Classical parallel or near-parallel flows of importance include wakes, pipe flows, jets, shear layers and boundary layers. There is strong evidence that in their turbulent state these flows can be described by similarity laws analogous to the theoretical similarity solutions of their laminar counterparts. Some of these "laws" are still evolving, but certain findings are established well enough to serve here as valid generalizations. One is that the scale Λ is geometrically related to the flow width h:

$$\Lambda = c_1 h, \; c_1 = \text{constant} \tag{9}$$

Another finding relates the r.m.s. velocity fluctuation u' with the "velocity scale" $u_e - u(o)$, representing the extremes in the velocity profile:

$$u' = c_2 (u_e - u(o)) \qquad , c_2 = \text{constant} \tag{10}$$

Utilizing a reference value ν_e for the viscosity, connected to ν via some temperature dependence

$$\frac{\nu}{\nu_e} = \left(\frac{T}{T_e}\right)^k \tag{11}$$

we can transform Equation (1) into:

$$Re_\Lambda = c_1\ h\ c_2\ (u_e - u(o))\ \left(\frac{T}{T_e}\right)^{-k} \frac{1}{\nu_e} \tag{12}$$

The width h scales with some characteristic dimension b of the flow and varies along the stream direction x, as does the so-called velocity defect

$$w \equiv \frac{u_e - u(o)}{u_e} = w(x) \tag{13}$$

so that

$$Re_\Lambda = C\ \left(\frac{u_e b}{\nu_e}\right)\ \frac{h}{b}\ (x)\ w(x)\ \left(\frac{T}{T_e}\right)^{-k} \tag{14}$$

Thus Re_Λ depends on the flow Reynolds number $Re_b \equiv u_e b/\nu_e$, on the dis- distance x from the flow origin (and on the flow geometry via the same functions h/b and w) and on the compressibility and heat-transfer, for which information resides in the temperature ratio.

Table I reproduces a list found in some elementary texts (References 13 and 14) with the addition of the Re_Λ behavior, at least with distance from the origin. For incompressible adiabatic flows ($T = T_e$) the self-preserving behavior of h/b and W is a well-known and usually simple function of X^n, where n takes on characteristic values depending on the flow [13]. For compressible and/or diabatic flows $k > o$ in Equation (14), generally causing Re_Λ to increase away from the flow origin, or at least to reinforce the increase caused separately by the growth of the flow width and to offset the decrease caused by the diminishing velocity defect. Thus, according to Table I, the axisymmetric incompressible jet has a constant Re_Λ along its length, but when the same jet is initially heated its Re_Λ increases in the downstream direction. As another example from Table I, compressibility or heating of a two-dimensional jet increases only the rate, and not the fact, of its streamwise increase of Re_Λ.

The present approach of finding flows, or segments of flows, where turbulence is permitted can be illustrated by computing Re_Λ from Equation (14) from any given flow. In Figure 1, such a computation is shown qualitatively for the flows of category II in Table I. The intercept of each curve with the threshold turbulence Reynolds number $Re_{\Lambda o}$ fixes the most forward position X_T in that flow where turbulence is allowed. As the Reynolds number Re_b increases X_T moves toward the flow origin. If

TABLE I

TURBULENCE REYNOLDS NUMBER BEHAVIOR
IN TYPICAL TURBULENT FLOWS

CATEGORY	TYPE FLOW	GEOMETRY	POWER n h/b	POWER n w	COMPRESSIBILITY STATUS	VARIATION OF Re_Λ AS X INCREASES
I	WAKE	2-D	1/2	-1/2	INCOMPRESSIBLE	CONSTANT
	JET	A/S	1	-1	INCOMPRESSIBLE	
	PIPE	A/S	0	0	INCOMPRESSIBLE	
II	WAKE	2-D	1/2	-1/2	COMPRESSIBLE	INCREASES
	JET	2-D	1	-1/2	INCOMPRESSIBLE	
	JET	2-D	1	-1/2	COMPRESSIBLE	
	JET	A/S	1	-1	COMPRESSIBLE	
	B. LAYER	2-D	1/2	0	INCOMPRESSIBLE	
	B. LAYER	2-D	1/2	0	COMPRESSIBLE	
	F.S. LAYER	2-D	1	0	INCOMPRESSIBLE	
	F.S. LAYER	2-D	1	0	COMPRESSIBLE	
III	WAKE	A/S	1/3	-2/3	INCOMPRESSIBLE	DECREASES
	WAKE	A/S	1/3	-2/3	COMPRESSIBLE	INCREASES/DECREASES

X_T is identified with the transition point or zone it follows that, for flows with increasing Re_Λ, (a) transition of the laminar flow will inevitably occur at some downstream point and, (b) the transition zone will advance upstream as the Reynolds number increases.

It can now be seen that for flows with constant Re_Λ (category I in Table I) the situation is drastically different because, in this case, the constant - Re_b curves (cf. Figure 1) will be straight lines parallel to the $Re_{\Lambda o}$ line. It follows that, (c) for flows of constant Re_Λ, the flow will be either completely laminar or completely turbulent from its origin onward depending on its Re_b.

The incompressible axisymmetric wake, according to Table I, belongs to a category with uniformity decreasing Re_Λ, and in this case the Re_b = constant curves analogous to those of Figure 1 will have a negative slope. It follows that, (d) for the axisymmetric incompressible wake, the end state of the flow will always be laminar and, (e) such wakes of originally high Reynolds number Re_b will experience a relaminarization process. Conclusion (d) does not change when compressibility is present, but in this case it is possible to have a wake experiencing transition downstream of the body followed by relaminarization some distance thereafter.

In the preceding, we progressed from the qualitative estimates of Re_Λ behavior listed on Table I to statements about transition, risking an extension of the necessary condition for the existence of turbulence, into a sufficient condition as well. The justification is that the rules (a)-(e) derived for the turbulence Reynolds number are overwhelmingly supported by experimental evidence on transition. For example, the fact that two-dimensional incompressible wakes are either completely laminar or completely turbulent is so commonplace that it seldom evokes inquiry [15]. It was not until the last two decades that the study of the compressible 2-D wake revealed the existence of a definite transition zone as equally commonplace [16]. Similarly, pipe flows do not possess a clear transition zone [17], in agreement with rule (a), above. More importantly, the forward movement of transition with increasing flow Reynolds number has been observed in all flows listed under Category II on Table I, in agreement with the present predictions. The tendency of the axisymmetric incompressible wake to relaminarize has appeared in the literature under the guise of the "final period" [5], while the tendency of its compressible counterpart to undergo transition followed by relaminarization has also been discussed in the past [12].

The precise cause of the apparent agreement between our threshold criterion and the observed behavior of transition is not clear, but it certainly encourages us to see if the agreement extends to the quantitative aspects of transition. Equations providing satisfactory quantitative agreement with transition phenomena in wakes and boundary layers have already been derived [1-3], and will now be sought below for the free shear layer.

5. TRANSITION IN THE FREE SHEAR LAYER

5.1 Definitions and Nomenclature

We are interested in predicting the location of laminar-turbulent transition along a shear layer separating two chemically homogeneous but otherwise arbitrary streams. Subscripts 1 and 2 are used to label the "fast" and "slow" sides respectively, i.e., $u_1 > u_2$ relative to a stationary observer. Since $P_1 = P_2$, the differences between the two streams can be characterized by any three parameters, here chosen to be λ, M, and T_{o2}/T_{o1} (see List of Symbols). Theoretical solutions for the asymptotic mean flow of these layers are available [18,19] for the laminar case and, within the assumption of an eddy viscosity, for the turbulent case as well. The available experimental data (ordinary or long-term averages) support the theory quite well so that the growth rates, which for example will be utilized below, can be considered well understood.

The object of our attention, the transition from a laminar to a turbulent FSL, is an experimental fact and a postulate of the discussion concerning Table I. It is important to the ideas expressed below to formalize the geometry of the transition zone as shown on Figure 2. Although the transition process occupies a finite zone of considerable length in reality, it is permissible to approximate it here with a certain hypothetical position (a "point") lying a distance X_T downstream of the flow origin. Because of the different growth rates of the laminar and turbulent FSL boundaries, it then follows that a layer thickness h_T at transition can be defined from the intersection of these boundaries. The virtual origin of turbulence then lies a distance x_o downstream of the actual origin and can be computed once X_T is known, making possible the computation of the turbulent FSL itself downstream of transition. The calculation of x_o is therefore an important by-product of this work, and will be discussed in Section 5.2.8.

It is important to make it clear at this point that the transition "point" is the intersection of the asymptotic laminar and turbulent boundaries, that is, of the boundaries defined according to the laminar and turbulent similarity solutions; in other words, the actual transition zone (shown by the fairing in Figure 2) is defined as the segment of the FSL linking the self-similar laminar and turbulent flows. In this way, we will be consistent with the computation of Re_Λ which will utilize the approximate formulas for the self-similar values of u' and Λ, as available. There will, of course, exist cases (e.g. transition very close to the laminar flow origin) where the laminar FSL will be too short to possess a self-similar growth. In cases such as a laminar flow originating from separation, too, it will be necessary to define the virtual origin of the laminar flow as well.

A second point regarding Figure 2 is that the FSL is pictured as symmetric about a plane passing through the dividing streamline. Actually, the distribution of flow properties is asymmetric in the general case, as can be verified by inspecting the theoretical results of both laminar and turbulent mixing layers.

Finally, the construction of Figure 2 represents the classic conception of mixing layers which ignores the more recent findings of Roshko and his coworkers [20], that low-speed laminar mixing, at least, occurs through a train of vortices reminiscent of the Karman vortex street behind a cylinder.

Note in Figure 2 that ξ $(= x - x_0)$ is the distance measured from the virtual origin of turbulence. The plan of the following Section is first to compute the transition distance x_{oT} from this origin, and then to convert x_{oT} to the actual transition distance X_T. This conversion will be done via the intermediate step of computing the layer thickness h_T at transition.

5.2 Transition Predictions

5.2.1 Method

The theoretical approach to predicting transition in the FSL is the same as utilized earlier by this author [1,4], for deriving analogous equations for the wake and boundary layer. The central statement of this method is that the turbulence Reynolds number

$$Re_\Lambda \equiv \frac{u'\Lambda}{\nu} \tag{1}$$

in the downstream portion of the turbulent flow following the transition zone, has to have a minimum value $Re_{\Lambda o}$. The mechanics of prediction then consist, first, of assuming that the particular flow under scrutiny is wholly turbulent; then, Re_Λ is computed along this hypothetically turbulent flow. The point along the flow where Re_Λ equals $Re_{\Lambda o}$ is the transition point, upstream of which Re_Λ is usually smaller than $Re_{\Lambda o}$. Since no turbulent flow can exist unless $Re_\Lambda > Re_{\Lambda o}$, this upstream region is laminar.

Thus, according to the above, the present task consists of computing the turbulence Reynolds number, given by Equation (1), along the FSL. This means that the fluctuation intensity u', scale length Λ and kinematic viscosity ν should be computed as a function of the distance x from the flow origin, going downstream. Before this computation is done below, however, it is necessary to clarify, or at least discuss, the following conceptual difficulty.

The quantity Re_Λ varies across the layer as well as with x, and since u' is zero outside the FSL and has a maximum in it, then Re_Λ will also have a maximum in it according to its definition (Equation (1)). The question now is, what value of Re_Λ is to be chosen at each x. If we choose the maximum Re_Λ, then we imply that the flow can locally sustain the turbulence if Re_Λ reaches $Re_{\Lambda o}$ at that point only. This is clearly awkward: assume, for example, that $Re_\Lambda = Re_{\Lambda o}$ at the center of the flow section; turbulence will then only be permitted in the exact center of the flow and not anywhere else, which hardly satisfies the definition of a turbulent flow.

In parallel work done by this writer to investigate transition in a boundary layer, the same question could not be circumvented, and the theory had to consider the lateral variation of Re_Λ at each x station. On the other hand, in applying the theory to wakes, [1], successful predictions were made using the Re_Λ magnitude in the center of the flow. Therefore, despite the misgivings of the preceding paragraph, we will here take the following position: if a turbulent FSL has a maximum Re_Λ equal to or larger than the threshold $Re_{\Lambda o}$, then that flow is permitted to be locally turbulent. If, however, conditions are such that Re_Λ at its maximum at some x is below $Re_{\Lambda o}$, turbulence is forbidden. Transition will be at the boundary between the permitted and forbidden portions of the FSL.

This postulate now clears the way for computing a unique $Re_\Lambda(x)$ for each given FSL. We know that u' will have a maximum on the dividing streamline (DSL); thus, all quantities appearing in Equation (1) must be computed there.

5.2.2 Calculation of the Turbulence Reynolds Number

The objective now is to compute the variation of Re_Λ for any turbulent shear layer, allowing for a wide variation of the FSL conditions such as M_1, λ and T_{02}/T_{01} (no gas composition differences are considered here; only homogeneous flows are discussed). In line with previous remarks, only the Re_Λ along the dividing streamline will be computed. Thus, for each turbulent FSL, a unique curve $Re_\Lambda(x)$ will be obtained; the point where $Re_\Lambda = Re_{\Lambda o}$ will be the "transition point." Thus, the transition distance x_{oT} (see Figure 2) will be expressed in terms of the FSL parameters:

$$x_{oT} = x_{oT}(M_1, \lambda, T_{o2}/T_{o1}) \qquad (15)$$

and some constants which will be discussed in due course. The parameters forming Re. in Equation (1) will now be evaluated one by one.

5.2.2A Kinematic Viscosity

The subscript convention, according to Figure 2, will be to use "1" for the faster and "2" for the slower stream, and subscript "DSL" for properties on the dividing streamline (DSL). Thus,

$$\nu_{DSL} = \left(\frac{T_{DSL}}{T_1}\right)^{k+1} \nu_1 \qquad (16)$$

where k, the temperature-viscosity exponent, is about 0.75 for air. The temperature ratio in this equation can then be found in the Appendix:

$$\frac{T_{DSL}}{T_1} = \frac{1}{2}\left(1 + \frac{\gamma-1}{2} M_1^2\right)\left(1 + \frac{T_{o2}}{T_{o1}}\right) - \frac{(\gamma-1)M_1^2}{2(1+\lambda)^2} \qquad (17)$$

5.2.2B Integral Scale

The integral scale Λ is perhaps the least known of the quantities needed; in contrast with the Crocco relation giving Equation (17), above, the scale will be only approximately estimated from experiments in boundary-layers [21], and wakes [22]. Thus, it is assumed that (a) Λ is constant across the FSL width and (b) Λ is proportional to the turbulent width h_t of Figure 2:

$$\Lambda = c_1 h_t \qquad (18)$$

The width h is known from the work of Ortwerth and Shine [23] and others:

$$h_t = \frac{\pi\lambda\xi}{\sigma_o} g(M_1) \qquad (19)$$

where the function $g(M_1)$ contains the "thickening" effect caused by the Mach number, and σ_o is the incompressible spreading parameter to be discussed farther below.

In this work, it was necessary to express $g(M_1)$ analytically so that transition calculations might be done. Calculated values are available from Ortwerth and Shine [23] and Oh [24], as well as experimental data from a number of sources (see Reference 25). The differences among these values of $g(M_1)$ are not significant, however, and it was decided to compromise by curve-fitting $g(M_1)$ into:

$$g(M_1) = 0.3 + 0.7 \exp\left(-0.064 M_1^{\,4}\right) \tag{20}$$

5.2.2C <u>Fluctuation Intensity</u>

According to Ortwerth [23], the dividing-streamline fluctuation intensity is:

$$u' = 0.16\ \Gamma (M_1)\ (u_1 - u_2) = 0.16\ \Gamma (M_1)\ \frac{2\lambda}{\lambda+1}\, u_1 \tag{21}$$

Like the function $g(M_1)$, $\Gamma (M_1)$ was for convenience approximated by

$$\Gamma (M_1) = \exp\left(-0.42 M_1\right) \tag{22}$$

5.2.2D <u>The Turbulence Reynolds Number</u>

If we combine the above equations into Equation (1), we obtain:

$$Re_\Lambda\ (\xi) = \left(\frac{u_1 \xi}{\nu_1}\right)\ \left[0.32\ C_1 \frac{\pi}{\sigma_o}\right]\ \ \Gamma (M_1) g(M_1)\ \left(\frac{T_1}{T_{DSL}}\right)^{k+1}\ \frac{\lambda^2}{\lambda+1} \tag{23}$$

The critical value $Re_{\Lambda o}$ can be used to form a constant

$$C \equiv \frac{Re_{\Lambda o}}{0.32\ C_1 \frac{\pi}{\sigma_o}} \tag{24}$$

Then the transition Reynolds number is, from (23):

$$Re_{xo} = \frac{C}{\Gamma(M_1) g(M_1)}\ \left(\frac{T_{dsL}}{T_1}\right)^{k+1}\ \frac{\lambda+1}{\lambda^2} \tag{25}$$

with $$Re_{xo} \equiv \frac{u_1 x_{oT}}{\nu_1} \tag{26}$$

x_{oT} = transition distance from the virtual origin of turbulence.

The above Reynolds number, based as it is on x_{oT} (see Figure 2), cannot be immediately identified with any physical transition length, since x_{oT} is not known "a priori". It is therefore plotted on Figures 3 and 4 more as a matter of interest than utility. The constant C will be discussed in Section 5.2.6.

5.2.3. The Transition Criterion Based on the Layer Thickness

More meaningful than the Reynolds number derived above is one based not on x_{oT} but on the idealized thickness h_T shown on Figure 2. According to eq. (19):

$$h_T = \frac{\sqrt{\pi}\lambda x_{oT}}{\sigma_o} g(M_1) \tag{27}$$

which can be considered to be either the thickness of the turbulent flow after a distance x_{oT} from the virtual origin, or that of the laminar flow at a distance x_T from the actual origin. Eliminating x_{oT} among equations (25), (26) and (27) we obtain:

$$Re_{hT} = \frac{u_1 h_T}{\nu_1} = \frac{C'}{\Gamma(M_1)} \left(\frac{T_{DsL}}{T_1}\right)^{k+1} \frac{\lambda+1}{\lambda} \tag{28}$$

with

$$C' = \frac{Re_{\Lambda o}}{0.32C_1} \tag{29}$$

Equation (28), which is plotted on Figures 5, 6, and 7, is somewhat easier to use than eq. (25) sinc the thickness h_T can be measured without exact knowledge of the actual flow origin or the virtual origin of the turbulence; the constant C' is related simply to C (compare equations (24) and (29)) and will be discussed in Section 5.2.6. Since eq. (28) has many common points with the final expression for the transition Reynolds number given further below, its discussion will be replaced (in Section 5.2.7.) by a discussion of the final expression. The latter substitutes the laminar wetted length x_T in place of h_T in eq. (28) or of x_{oT} in eq. (25). To do that, it is necessary to first consider briefly the equations describing the development of a laminar free shear layer.

5.2.4. The Laminar Free Shear Layer Width

The laminar shear layer development, following the solutions of Goertler for incompressible flows (Reference 26) has been solved for the arbitrary homogeneous case by several workers including Crane (Reference 18), Mills (Reference 19), Moeny (Reference 27), and others. In the case of Crane and Mills the solutions are of the similarity type for arbitrary M_1, λ and T_{02}/T_{01};

calculating $h_1(x)$ from their results is difficult, however, since the latter involve numerical computations although the solutions themselves are analytic. In this report, therefore, we will use the approximate asymptotic formulas for $h_1(x)$ derived by Moeny (Reference 27) following the integral method of Dewey and Kubota (Reference 28).

Moeny derives the following approximate asymptotic expressions for two "half-layers" δ_1 and δ_2 which make up the shear layer:

$$\delta_1 \simeq \left[\frac{4(1+K)}{\frac{K}{3} + \frac{R_1}{5} + \frac{2}{15}} \right]^{1/2} \frac{x}{\sqrt{Re_{1x}}} \tag{31}$$

$$\delta_2 \simeq \left[\frac{4(1+K)}{\frac{R_1}{3} + \frac{K}{5} + \frac{2}{5} R_1 K} \right]^{1/2} \frac{x}{\sqrt{Re_{1x}}} \tag{32}$$

where:

$$K \equiv \frac{\delta_2}{\delta_1} = \frac{u^* - R_1}{1 - u^*} = \frac{-3(R_1 - 1) + [33R_1^2 + 34R_1 + 33]^{1/2}}{2(3 + 2R_1)} \tag{33}$$

$$R_1 = \frac{u_2}{u_1} = \frac{1-\lambda}{1+\lambda} \tag{34}$$

$$u^* = \frac{K + R_1}{1 + K} \tag{35}$$

$$\delta_1 + \delta_2 = \delta \tag{36}$$

and where the nomenclature is otherwise the same as in this report. The physical asymptotic FSL thickness then is:

$$h_1 = \left[\left(1 + \frac{\gamma - 1}{2} M_1^2\right) \left[\frac{u^*(1 - R_3) - 3R_1 + 2 + R_3}{3(1 - R_1)} \right] - \frac{(\gamma - 1)}{2} M_1^2 \left[\frac{3u^{*2} + 4u^* + 8}{15} \right] \right] \delta_1 +$$

$$+ \left[\left(1 + \frac{\gamma-1}{2} M_1^2\right) \frac{1}{1-R_1} \left[\frac{u^*}{3}(1-R_3) - \frac{R_1}{3}(1+2R_3) + R_3 \right] - \right.$$

$$\left. - \frac{(\gamma-1)}{2} M_1^2 \left[\frac{3u^{*2} + 4R_1 u^* - 8R_1}{15} \right] \right] \delta_2 \qquad (37)$$

where $R_3 = T_{02}/T_{01}$.

Computations done with eq. (37) are shown on Figures 8 and 9. For adiabatic and "heated" flows (T_{02}/T_{01} = 1 and 3, for example) the behavior of the thickness h_1 is normal, as attested by Figure 8; increases in λ, M_1 and T_{02}/T_{01}, whether separately or in combination, cause a thickening of the layer. The situation is altogether different for the case of cooling (for example T_{02}/T_{01} = 1/3 shown on Figure 9). Here the thickness increases with increasing M_1 only for λ larger than about 0.2; it actually decreases with increasing M_1 for $\lambda < 0.2$. However, we note from Figure 9 that this decrease is arrested when the curves cross the dashed boundary shown in the Figure. This boundary encloses the region which, as explained in the Appendix, involves $T_{DSL} < 0$ and/or $T_1 < 0$ (the latter being more restrictive) caused by the simultaneous prescription of M_1, λ, and T_{02}/T_{01}. In other words, for this region the FSL is unrealistic and will not be considered in further computations.

In passing, note that for incompressible layers (M_1 = 0) the thickness is shown on the inset of Figure 8. Also, when the two streams become equal (λ = 0, T_{02}/T_{01} = 1) the FSL thickness approaches, from eq. (31)-(37), the limit:

$$\frac{h_1}{x} \sqrt{Re_{1x}} = 4\sqrt{3} = 6.93.... \qquad (38)$$

which is shown on Figure 8.

5.2.5. <u>The Criterion Based on Distance From the Origin</u>

The results of Sections 5.2.3. and 5.2.4. now enable us to compute the desired transition Reynolds number

$$Re_{xT} = \frac{u_1}{\nu_1} x_T \qquad (39)$$

where x_T is the distance between the transition location and the flow origin, according to Figure 2. By equations (31)-(37) the relation between x_T and h_T is:

$$\frac{h_T}{x_T}\sqrt{Re_{xT}} \equiv \frac{h_T}{x_T}\left[\frac{u_1}{\nu_1}x_T\right]^{1/2} = G(\lambda, M_1, \frac{T_{02}}{T_{01}}) \tag{40}$$

and G is the function already plotted on Figures 8 and 9. At the same time, we saw in Section 5.2.3. that:

$$Re_{hT} \equiv \frac{u_1}{\nu_1} h_T = \frac{C'}{\Gamma(M_1)} \left(\frac{T_{DSL}}{T_1}\right)^{k+1} \frac{\lambda+1}{\lambda} \tag{41}$$

If h_T is eliminated between equations (40) and (41), we finally obtain:

$$\frac{Re_{xT}}{C''} \equiv \frac{1}{C''}\frac{u_1}{\nu_1}x_T = \frac{1}{\Gamma^2 G^2}\left(-\frac{T_{DSL}}{T_1}\right)^{2(k+1)} \left(\frac{\lambda+1}{\lambda}\right)^2 \tag{42}$$

with

$$C'' \equiv C'^2$$

$$k = 0.75 \text{ (for air)}$$

As before, Γ and T_{DSL}/T_1 can be found from equations (17) and (22) respectively. The constant C", related to C via equations (24) and (29), will be discussed below.

Equation (42) is plotted in Figures 10, 11 and 12 vs. λ, with M_1 as a parameter and for three typical values of T_{02}/T_{01}. For the adiabatic and heated FSL (T_{02}/T_{01} = 1,3 respectively) the results show a very rapidly increasing transition Reynolds number as λ decreases; this is fully expected since Re_{xT} should be infinite when $\lambda = 0$. The transition Reynolds number also increases very fast as M_1 increases. The increase with λ is fastest (of order λ^{-2}) at the smallest M_1 and λ_1 and slower at the larger M_1 and λ. The dependence on M_1 is typical of the well-known stabilization of all parallel shear flows as M_1 increases.

The plots of Figures 10 and 11, and especially 12, show that transition moves forward as the "cooling" increases, i.e. as T_{02} becomes smaller relative to T_{01}; the shear layer, therefore is "wake-like" in the sense that transition moves forward with cooling (Reference 29); the opposite is true, of course, for boundary layers. However, the behavior of Re_{xT} is somewhat irregular when T_{02}/T_{01} = 1/3, as shown on Figure 11, when $M_1 > 1$. For high Mach numbers, especially, Re_{xT} becomes rather insensitive to λ. The termination points for the $M_1 > 1$ curves on Figure 11 define the "forbidden" region for cooled shear layers corresponding to the comments relating to Figure 9.

It should be noted that for incompressible, adiabatic layers ($M_1 = 0$, $T_{02}/T_{01} = 1$) equation (42) becomes:

$$\frac{Re_{xT}}{C''} = \frac{1}{G^2} \left(\frac{\lambda+1}{\lambda} \right)^2 \tag{43}$$

which is plotted on Figure 10.

5.2.6. Evaluation of the Numerical Constants

Accurate knowledge of the constituents of the constant C of equation (25) are needed for numerical application of the transition prediction (eq. (42)). In previous work (see Discussion in Reference 1) the threshold turbulence Reynolds number $Re_{\Lambda o}$ had been found to be approximately 15. Use of the same value in eq. (24) is highly desireable because it will test, in the long run, the general validity of the present approach to the transition problem.

No information seems to exist for shear layers on the constant c_1 relating the integral scale and the layer width (cf.eq. (18)). In fact, what is needed in the value or variation of c_1 as a function of M_1, λ, T_{02}/T_{01} etc. including its change, if any, across the layer. This serious shortcoming will be met here by assuming $c_1 = 0.2$, a value deriving from wake (Reference 22) and boundary layer studies (Reference 21).

The factor 0.32 in eq. (24) derives from the magnitude, measured by several workers, of u' at its maximum point in the shear layer (the usual finding is $0.16(u_1-u_2)$, and here a factor of 2 is added by the algebraic sequence of events). There is no information assuring us that this value is unaffected by heat transfer ($T_{02}/T_{01} \neq 1$). Actually, experimental data on u' are very scarce for $M_1 > 0$, as well as for sufficient number of λ values; this issue is certainly far from settled.

Using the most commonly known values of c_1, $Re_{\Lambda o}$, etc. (the spreading parameter $\sigma_o = 11.3$) we can then compute

$$C \equiv \frac{Re_{\Lambda o}\ \sigma_o}{.32\ C_1} = \frac{15 \times 11.3}{0.32 \times 3.14 \times 0.2} \simeq 843 \tag{44}$$

It then follows that the constant used for finding the transition Reynolds number based on thickness of eq. (28) is:

$$C' = \frac{15.5}{0.32} 5 = 234 \tag{45}$$

while that used to find the transition Reynolds number based on the actual physical length, in eq. (42) is:

$$C'' = C'^2 = 54{,}760 \qquad (46)$$

5.2.7. The Virtual Origin of the Turbulent Flow

As already mentioned, knowledge of the virtual origin of the turbulent FSL is needed to compute the growth of the latter, if and when the layer itself experiences transition. Specifically, we are interested in knowing the distance x_{oT} of Figure 2 once we have established x_T as was just done in the previous section. This can be done directly from eqs. (25) and (42):

$$\frac{x_{oT}}{x_T} = \frac{u_1}{\nu_1}\,\frac{X_{oT}}{u_1}\,\frac{\nu_1}{x_T} = \frac{Re_{xo}}{Re_{xT}} = \frac{C}{C''}\left(\frac{Re_{xo}}{C}\right)\left(\frac{C''}{Re_{xT}}\right) \qquad (47)$$

The ratio C/C" is given in the previous section as 0.0154.

Computations with eq. (47) are shown on Figures 13 and 14. For the incompressible, adiabatic case the ratio x_{oT}/x_T is constant at about 0.74; that is, the turbulent flow originates at a hypothetical point lying downstream of the actual flow origin, about 1/4 of the distance between the latter and the transition point. Generally, too, the results show that the higher the Mach number the closer the virtual origin lies to the transition point. The inference is that the actual transition zone itself shrinks greatly at the very large Mach numbers.

5.2.8. Comparison With Experiment

There are no other theoretical approaches to the FSL transition problem for comparison with the present approach. Earlier statements found in the literature (Reference 30) tend to associate the Re_{xT} with $1/\lambda$:

$$Re_{xT} \sim \frac{1}{\lambda} \qquad (48)$$

As already discussed in Section 5.2.5. in connection with Figure 10, the present approach indicates a much steeper rise in Re_{xT} as λ decreases, except for high M_1 and possibly for low T_{02}/T_{01}. For example, whereas (48) implies an increase in Re_{xT} by a factor of 100 between $\lambda = 1$ and 0.01 at $M_1 = 0$, $T_{02}/T_{01} = 1$, the present approach, by eq. (42), gives an increase of about 5,000. In addition, the formulas derived here give explicitly the dependence of Re_{xT} on M_1 and T_{02}/T_{01} for the first time.

Comparison with experiment should, in principle, be straightforward, but most experiments with mixing layers involve pre-transitional flows with unknown or unclear laminar flow origin; such would be, for example, the case of two streams initially separated by a partition, which mix together beyond the trailing edge of the partition. The virtual origin of the laminar flow in such experiments can be established based on details of the observed flow field rarely presented in the literature. Or, one could compare such test data with the present formulation of transition based on thickness (Section 5.2.3.) provided that the experimental paper gives a detailed account of the pre-transitional (laminar) growth of the shear layer.

In the meantime, it is possible to compare eq. (42) with data from experiments producing shear layers from the intersection of shock waves, as reported by Crawford (Reference 31), Birch and Keyes (Reference 30), and this author (Reference 4). These experiments define the laminar flow origin quite precisely although they are usually restricted to adiabatic flows. This comparison is shown on Figures 15 and 16. According to the former the data of Birch and Keyes are satisfactorily represented by the theory, but not so the data of this author, which are lower than the theory by a factor of as much as two. On Figure 16 it is seen that Crawford's increasing Re_{xT} as M_1 increases, although not at the rate or to the magnitude given by the theory.

The experimental results quoted above are obscured by a feature which generates the vertical bars plotted on Figures 15 and 16, in lieu of points. All data shown have been found to depend on the flow unit Reynolds number, which is usually the lowest at the bottom of each bar and highest at its top. This influence apparently is universal for all experiments shown; it seems smallest in the Birch-Keyes tests and largest in the test of this author at AEDC (Reference 4) where x_T was observed actually to move downstream as Re' was increases. There is no explanation for this unit Reynolds number effect although the trend is identical with the observed increase of boundary-layer transition Reynolds number with unit Reynolds number. It would be pure speculation to support that better agreement with the present theory would be obtained if the test unit Reynolds number could be infinitely increased; however, more experimenta' data are obviously needed to examine and verify this effect.

Although the numerical agreement with data is only fair, the qualitative trends of the increase of Re_{xT} with λ and M_1 is clear. The overwhelming fact, of course, is that the information needed to quantify this approach is not yet available. Reading through Section 5.2.6. one is impressed with the severity of the approximations made in order to evaluate C, C' and C", for example. The data utilized to form these constants (e.g. the scale length, fluctuation magnitude, etc.) is extremely maeager. Coupled with the inadequacies of the transition data described above, one is forced to withhold judgement on the theory until data become available - both for the ingredients of C and for comparison with the transition predictions.

6. CONCLUSIONS AND RECOMMENDATIONS

The necessary threshold for turbulence preservation in a homogeneous free-shear layer has been identified with the transition condition, and a calculation of transition Reynolds numbers have been made for layers or arbitrary jump conditions.

The transition Reynolds number has been found to increase very rapidly as the fast-side Mach number increases and as the velocity difference (jump) decreases. It also increases, although less rapidly, as the total temperature of the slow side increases. In addition, computations of the transition Reynolds number based on thickness have been done, as well as of the location of the virtual origin of turbulence. For incompressible, adiabatic shear layers, for example, this origin lies at one-quarter the distance from the actual flow origin to the transition station.

Numerical computations of the transition Reynolds number have been done using identical criteria as in earlier reports on transition in wakes and boundary layers. Although these inputs are considered still incomplete, they result in good qualitative and fair quantitative agreement with the theory. It should be stressed that the incomplete state of the computations is caused by the absence of precise measurements of "universal" turbulence properties.

The following are recommended steps to improve and expand the present work:

1) Experimentally, the observed dependence of Re_{xT} on the unit Reynolds number must be first verified, preferably with non-optical techniques such as hot-wire anemometry.

2) The present theory must be put to test by measuring Re_{xT} for as many combinations of λ, M, and T_{02}/T_{01} as practical.

3) On a theoretical basis, the relevant configuration of interest is not the slipstream with well-defined origin, but the shear layer coming off the trailing edge of a partition. For that case the present formulas must be modified to account for the hypothetical origin of the separated laminar boundary layer.

4) The present formulation must be extended to the heterogeneous mixing case (two dissimilar fluids).

APPENDIX A

THE DIVIDING-STREAMLINE TEMPERATURE IN SHEAR LAYERS ACCORDING TO THE CROCCO RELATION

The objective of this Appendix is to derive an expression for the static temperature T_{DSL} on the dividing streamline, which accounts for Mach number and speed ratio variation from low to high levels, as well as arbitrary total temperature differences between the two streams. Excepting differences in molecular composition, this would then provide the information needed to encompass all conceivable physical ranges of free shear layers.

Our task is, actually, to simplify and exploit the temperature-velocity relation ("Crocco relation") presented by Shapiro (Ref. 32), Korst and Chow (Ref. 33) and others:

$$\frac{T-T_1}{T_1} = f(M_1)\left[1-\left(\frac{u}{u_1}\right)^2\right] + \left[\frac{1-\frac{T_2}{T_1}}{1-\frac{u_2}{u_1}} + f(M_1)\left(1+\frac{u_2}{u_1}\right)\right]\left(\frac{u}{u_1}-1\right) \quad (A.1)$$

The objective here is to evaluate this formula at the dividing streamline (or "DSL"):

$$\frac{u_{DSL}}{u_1} = \frac{1}{2}\left(1+\frac{u_2}{u_1}\right) \quad (A.2)$$

and express the result in terms of M_1, λ and T_{02}/T_{01}. Note that

$$f(M_1) \equiv \frac{\gamma-1}{2} M_1^2 \quad (A.3)$$

To do this, note that

$$T_1 = T_{01} - \frac{u_1^2}{2c_p} \quad (A.4)$$

$$T_2 = T_{02} - \frac{u_2^2}{2c_p} \quad (A.5)$$

Folding the latter two equations into (A.1) we obtain, after some algebra, the following two alternative equations:

$$\frac{T_{DSL} - T_1}{T_1} = f(M_1)\frac{\lambda^2}{(1+\lambda)^2} - \frac{1}{2}\left(1 - \frac{T_2}{T_1}\right) \qquad (A.6)$$

$$\frac{T_{DSL} - \bar{T}}{T_1} = f(M_1)\left(\frac{\lambda}{1+\lambda}\right)^2 \qquad (A.7)$$

with

$$\bar{T} \equiv \frac{T_1 + T_2}{2} \qquad (A.8)$$

These equations are still unsatisfactory because they do not contain the ratio T_{02}/T_{01} explicitly; further manipulation produces the desired result:

$$\frac{T_{DSL}}{T_1} = \frac{1}{2}\left(1 + \frac{\gamma-1}{2}M_1^2\right)\left(1 + \frac{T_{02}}{T_{01}}\right) - \frac{(\gamma-1)M_1^2}{2(1+\lambda)^2} \qquad (A.9)$$

In equation (A.9) the parameters M_1, λ and T_{02}/T_{01} are independent, and any set of them should define a unique T_{DSL}/T_1 value. Physically speaking, however, there is an exception made when the second term on the r.h.s. of (A.9) exceeds the first which, it will be noted, can happen expecially if $T_{02}/T_{01} << 1$. In this case $T_{DSL} < 0$, a clearly impossible (but algebraically permitted) result. There are, therefore, minimum allowed values of T_{02}/T_{01} which, combined with any pair of prescribed M_1, λ values, will give $T_{DSL} > 0$ according to (A.9), and these are plotted in Figure 17. An additional, but similar, restriction on T_{02}/T_{01} arises when we require that in the "slow" stream (subscript "2") the temperature $T_2 > 0$. This criterion can be derived from eq. (A.7) and (A.8) and is plotted on the same figure. The criterion required to keep $T_2 > 0$ is, as Figure 17 shows, more restrictive than that requiring $T_{DSL} > 0$; that is, the latter criterion can be ignored so long as the former is accounted for. Thus, according to Figure 17, if we hypothesize a FSL with $M_1 = 3$ and $\lambda = 0.1$, say, then we can prescribe to this flow any T_{02}/T_{01} larger than 0.42 or so. Values of T_{02}/T_{01} less than that will create a physically unattainable flow. Thus, equation (A.9) subject to the restrictions of Figure 17 is the necessary tool for computing the kinematic viscosity entering the transition formula in the text.

We will forego demonstrating the lateral variation of temperature across the FSL according to (A.1), since such plots are relatively easy to do. It is, however, important to keep in mind that there are values of T_{02}/T_{01} for which T does not vary monotonically from T_1 to T_2. This can be seen by noting that

$$\frac{T_2}{T_1} = \left[1 + \frac{\gamma - 1}{2} M_1^{\,2} \right] \frac{T_{02}}{T_{01}} - \frac{\gamma - 1}{2} M_1^{\,2} \left(\frac{1 - \lambda}{1 + \lambda}\right)^2 \qquad (A.10)$$

and plotting $(T - T_1)/T_1$ vs. η, where as usual:

$$\frac{u}{u_1} = \frac{1}{1 + \lambda} \left[1 + \lambda\cos\eta \right] \qquad (A.11)$$

The result will show that, especially for large M_1 and λ and for $T_{02}/T_{01} < 1$, T arrives at a maximum between the two streams. The physical reason, of course, is that as the fast stream slows down to match the speed of the slow one, it experiences an isentropic temperature rise. In such cases the temperature profile resembles, as it should, a cold-wall supersonic boundary layer.

This parenthetic remark was made to prepare the user of eq. (A.9) for occasional "odd" behavior of T_{DSL}, such as an actual decrease for certain conditions illustrated on Figure 18 on which eq. (A.9) is plotted. Such behavior, setting in for $T_{02}/T_{01} < 1$, will have consequences in the transition predictions found in the text.

REFERENCES

1. Demetriades A.: "Transition To Turbulence In Two-Dimensional Wakes," AIAA J. vol. 16, No. 6, June 1978, pp. 587-591.

2. Demetriades A.: "Interim Progress Report: Stability, Transition And Turbulence In Mixing Layers And Adjacent Streams," Aeronutronic Publication NO. U-6488, Newport Beach, CA, October 1978.

3. Demetriades A.: "Consequences of A Necessary Threshold For Boundary-Layer Transition," submitted for publication to the AIAA J., 1979.

4. Demetriades A.: "Transition In Free Shear Layers," Aeronutronic Report No. U-6573, Newport Beach, CA, December 1979.

5. Townsend A. A.: "The Structure of Turbulent Shear Flow," Cambridge University Press, Cambridge, 1956.

6. Hinze J. O.: "Turbulence," McGraw-Hill Book Co., New York, NY, 1959.

7. Finson M. L.: "Hypersonic Wake Aerodynamics at High Reynolds Numbers," AIAA Paper 72-701, New York, NY, 1972.

8. Batchelor G. K. and Townsend A. A.: "Decay of Turbulence In The Final Period," Proc. Roy. Soc. A 194, 1948, p. 527.

9. Compte-Bellot G. and Corrsin S.: "The Use of A Contraction To Improve The Isotropy of Grid-Generated Turbulence," JFM vol. 48, 1971, p. 273.

10. Uberoi M. S. and Freymuth P.: "Spectra of Turbulence In Wakes Behind Circular Cylinders," Phy. of Fl., vol. 12, No. 7, July 1969, pp. 1359-1363.

11. Ortwerth P. J.: Private communications 1977-1979.

12. Lees L.: "Hypersonic Wakes And Trails," AIAA J. vol. 2, No. 3, March 1964, pp. 417-428.

13. Schlichting H.: "Boundary-Layer Theory," McGraw-Hill Book Co., New York, 1979.

14. Lin C. C. (Ed.): "Turbulent Flows And Heat Transfer," vol. 5, High Speed Aero. & Jet Prop. Series, Princeton University Press, Princeton, NJ, 1959, Ch. 5.

15. Roshko A.: "On The Development of Wakes From Vortex Streets," NACA TR 1191, Washington, D. C., 1954.

16. Demetriades A.: "Some Hot-Wire Anemometer Measurements In A Hypersonic Wake," Proc. of the 1961 HTFMI, Stanford University Press, 1961, p. 1.

17. Rotta J.: "Experimenteller Beitrag Zur Entstehung turbulenter Stromung im Rohr," Ing. Arch., Vol. 24, 1956, pp. 258-281.

18. Crane L. J.: "The Laminar and Turbulent Mixing of Jets of Compressible Fluid. Part II: The Mixing of Two Semi-Infinite Streams," JFM vol. 3, 1957, p.81.

19. Mills R. D.: "Numerical And Experimental Investigations of The Shear Layer Between Two Parallel Streams," J.F.M. vol. 33, part 3, 1968, pp. 591-616.

20. Roshko A.: "Structure of Turbulent Shear Flows: A New Look," AIAA Paper 76-78, Washington D. C., 1976.

21. Laderman A. J. and Demetriades A.: "Mean and Fluctuating Flow Measurements In The Hypersonic Boundary Layer Over A Cooled Wall," JF, vol. 63, part 1, 1974, p. 121.

22. Demetriades A.: "Turbulence Measurements In An Axisymmetric Turbulent Wake," Phy. of Fl., vol. 11, No. 9, September 1968, p. 1841.

23. Ortwerth P. J. and Shine A. J.: "On The Scaling of Plane Turbulent Shear Layers," Laser Digest, AFWL-TR-77-118, Spring 1977, p.115.

24. Oh O. H.: "Analysis of Two-Dimensional Free Turbulent Mixing," AIAA Paper 74-594, New York, NY, 1974.

25. Ikawa H.: "Turbulent Mixing Layer Experiment In Supersonic Flow," Ph.D. Thesis, California Institute of Technology, G.A.L.C.I.T., Pasadena, CA, 1973.

26. Gortler H.: "Berechnung von Aufgaben der freien turbulenz auf Grund eines neuen Naherungsansatzes," ZAMM vol. 22, 1942, pp. 244-254.

27. Moeny W.: Private communications 1979.

28. Kubota T. and Dewey C. F. Jr.: "Momentum Integral Methods for the Laminar Free Shear Layer," AIAA J. vol. 2, No. 4, April 1964, pp. 625-629.

29. Demetriades A.: "Heat Transfer Effects on Supersonic Wake Transition," Phy. of Fl., vol. 13, No. 1, January 1970, pp. 204-206.

30. Birch S. F. and Keyes J. W.: "Transition In Compressible Free Shear Layers," J.S.R. vol. 9, No. 8, August 1972, p. 623.

31. Crawford D. H.: "Investigation of The Flow Over A Spiked-Nose Hemisphere-Cylinder At A Mach Number of 6.8," NASA TN D-118, Washington, D. C., 1959.

32. Shapiro A. H.: "The Dynamics And Thermodynamics of Compressible Fluid Flow," The Ronald Press Co., New York, 1954, Vol. II.

33. Korst H. H. and Chow W. L.: "On The Correlation of Analytical And Experimental Free Shear Layer Similarity Profiles By Spread-Rate Parameters," J. of Basic Eng., ASME Transactions, Paper 70-WA/FE-12.

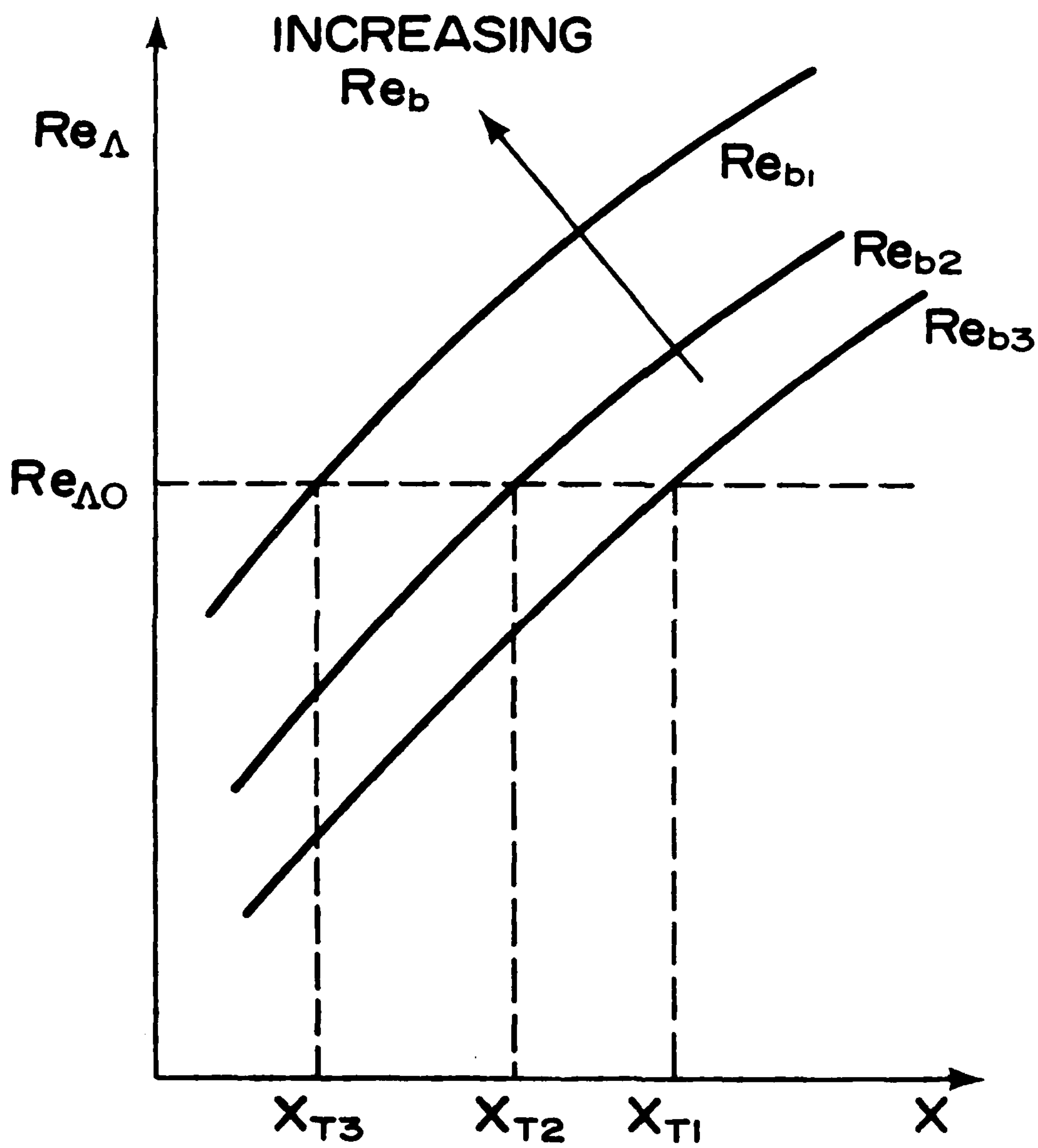

Figure 1. Movement of the "transition point" x_T when the flow Reynolds number Re_b increases, for flows with turbulence Reynolds numbers increasing in the downstream direction.

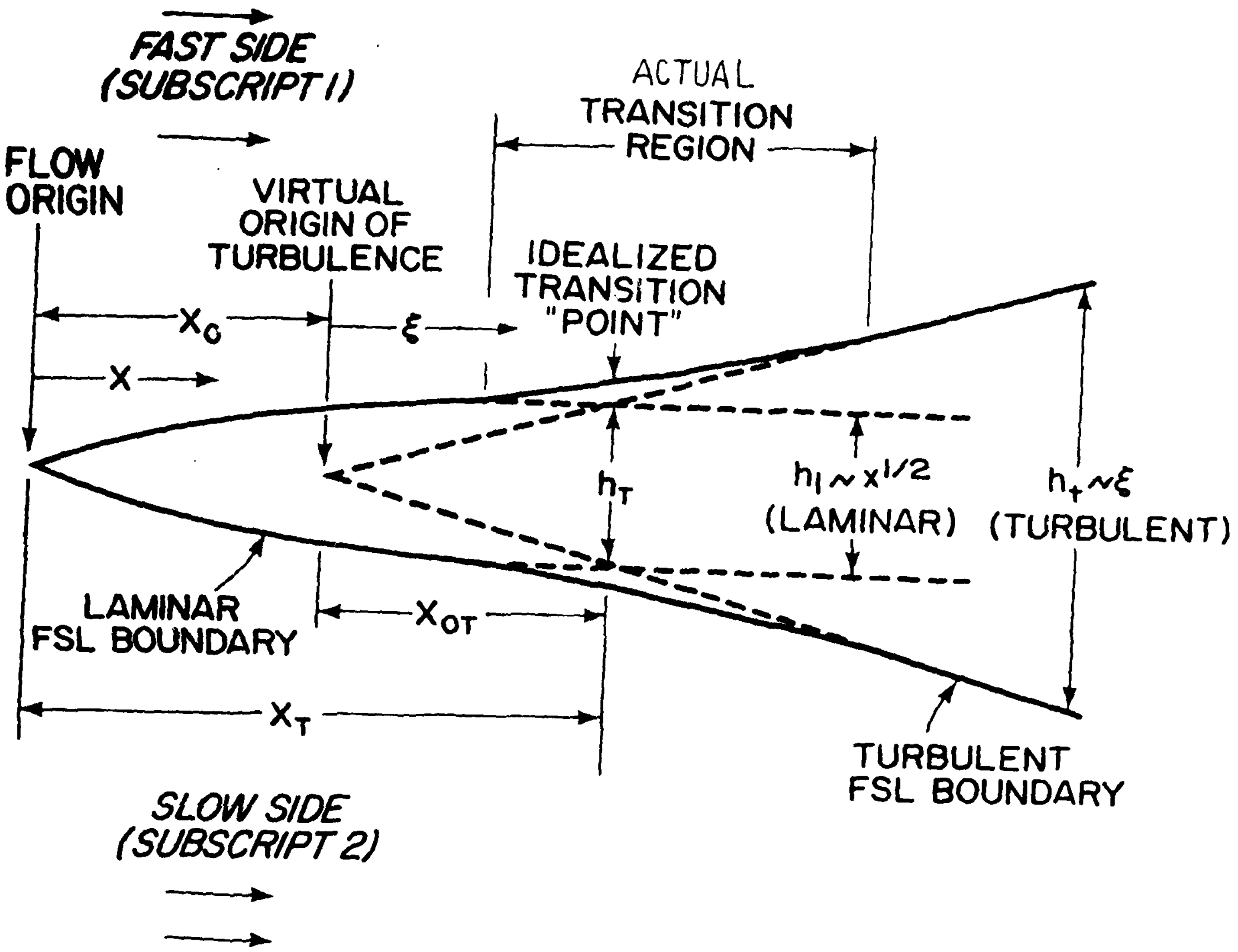

Figure 2. Flow-field definition.

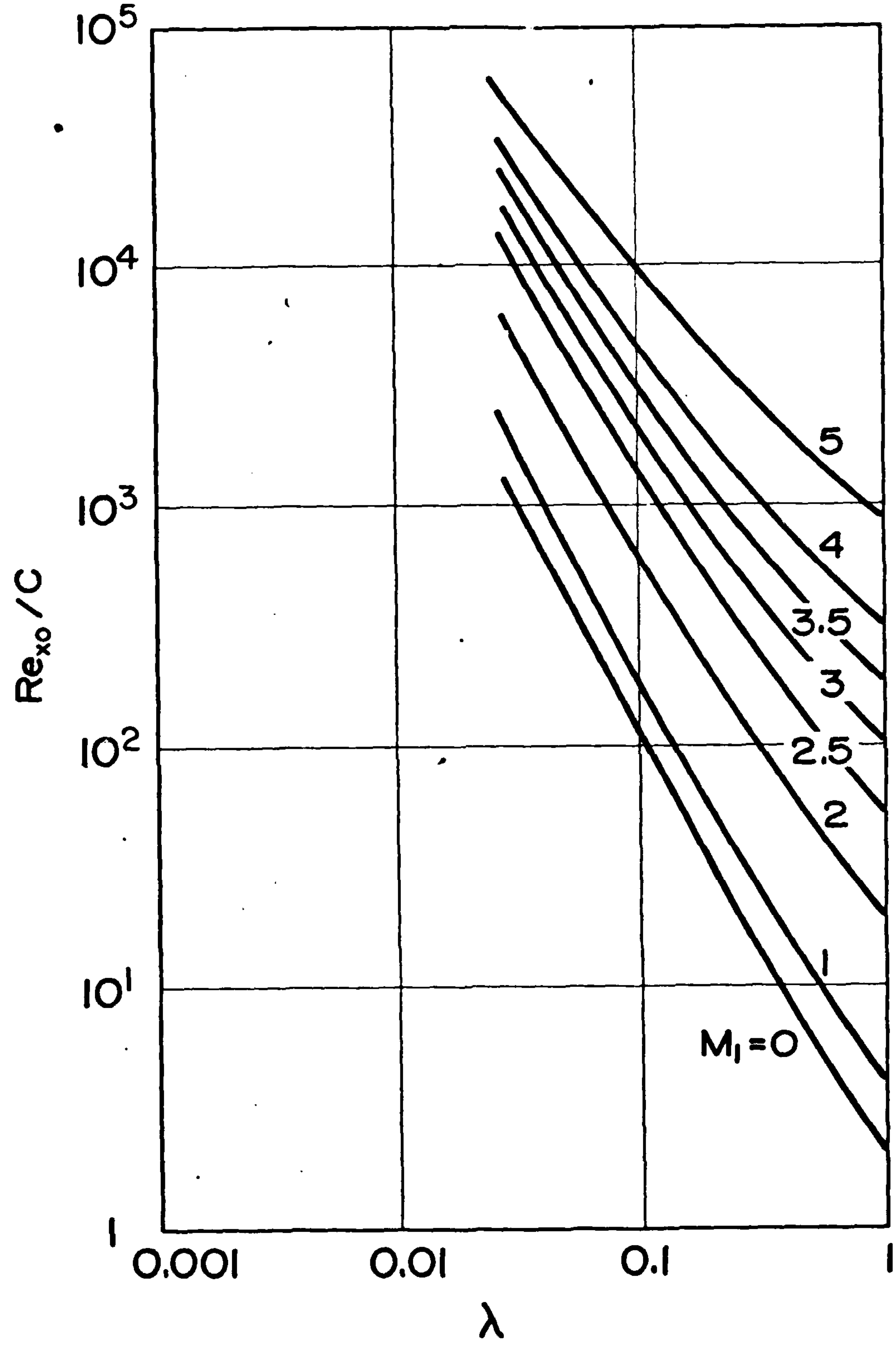

Figure 3. Transition Reynolds number based on the distance from the virtual origin of turbulence (adiabatic case).

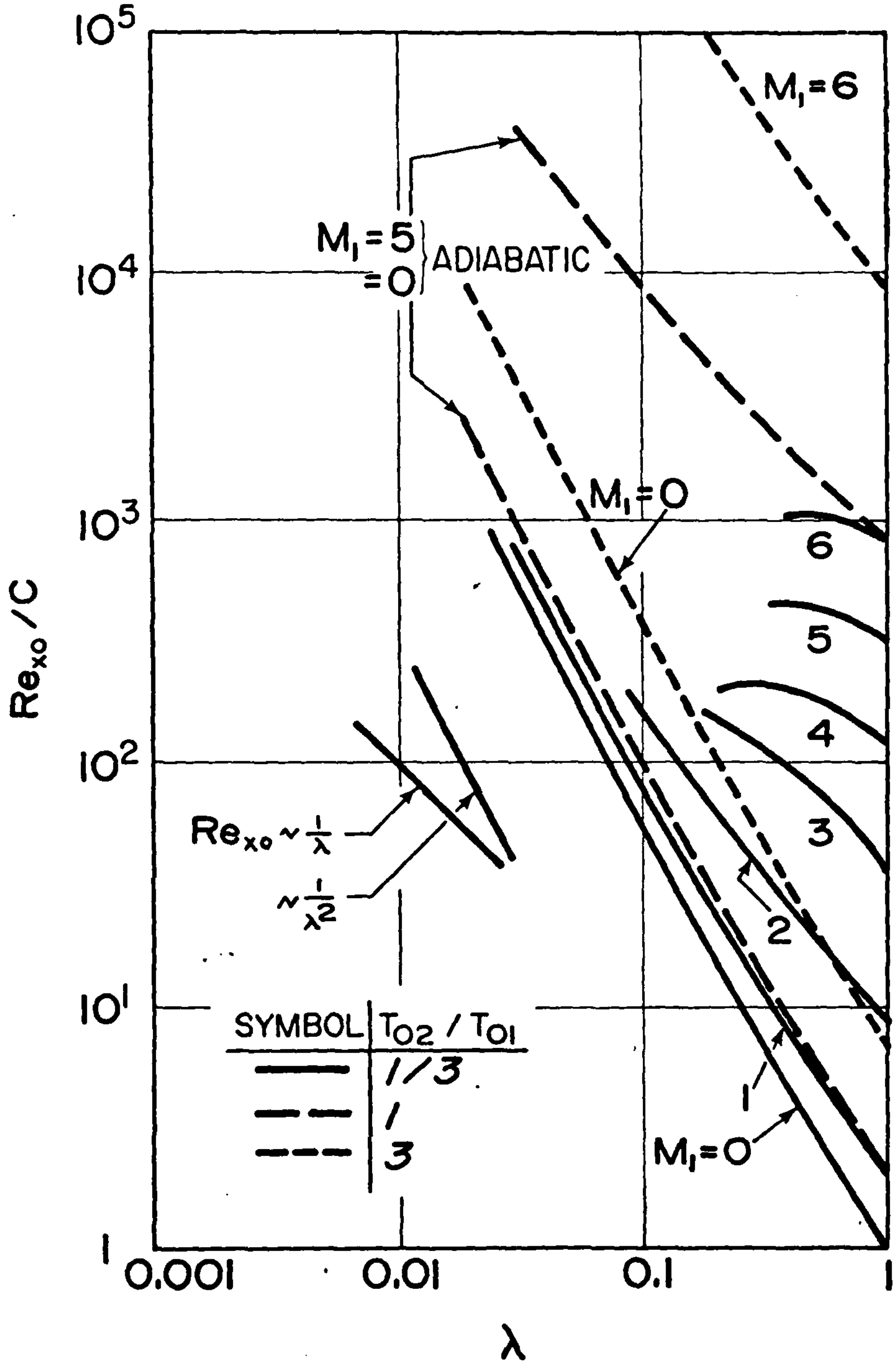

Figure 4. Transition Reynolds number based on the distance from the virtual origin of turbulence, with and without heat transfer.

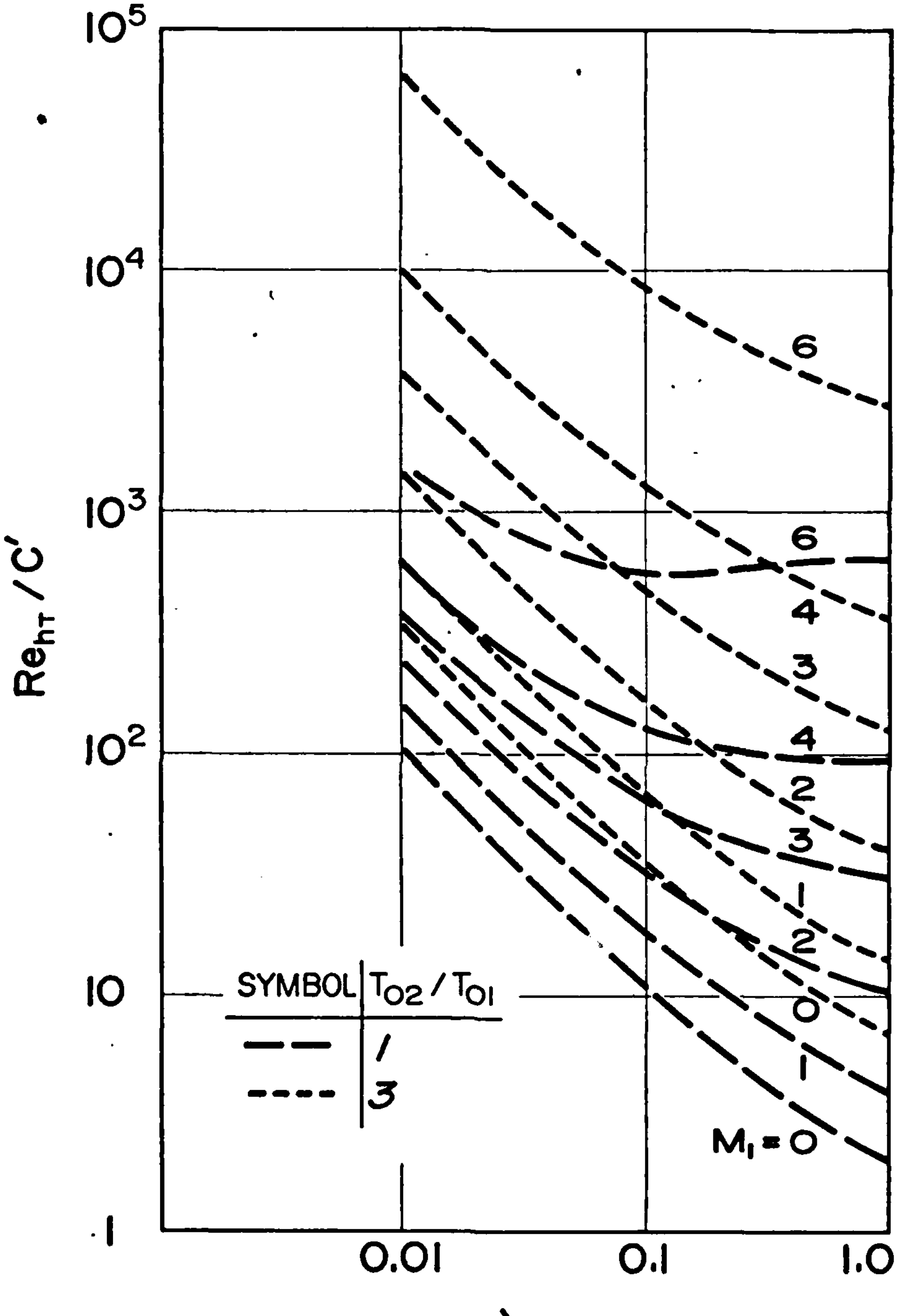

Figure 5. Transition Reynold number based on the FSL thickness at transition, for the adiabatic and heated cases.

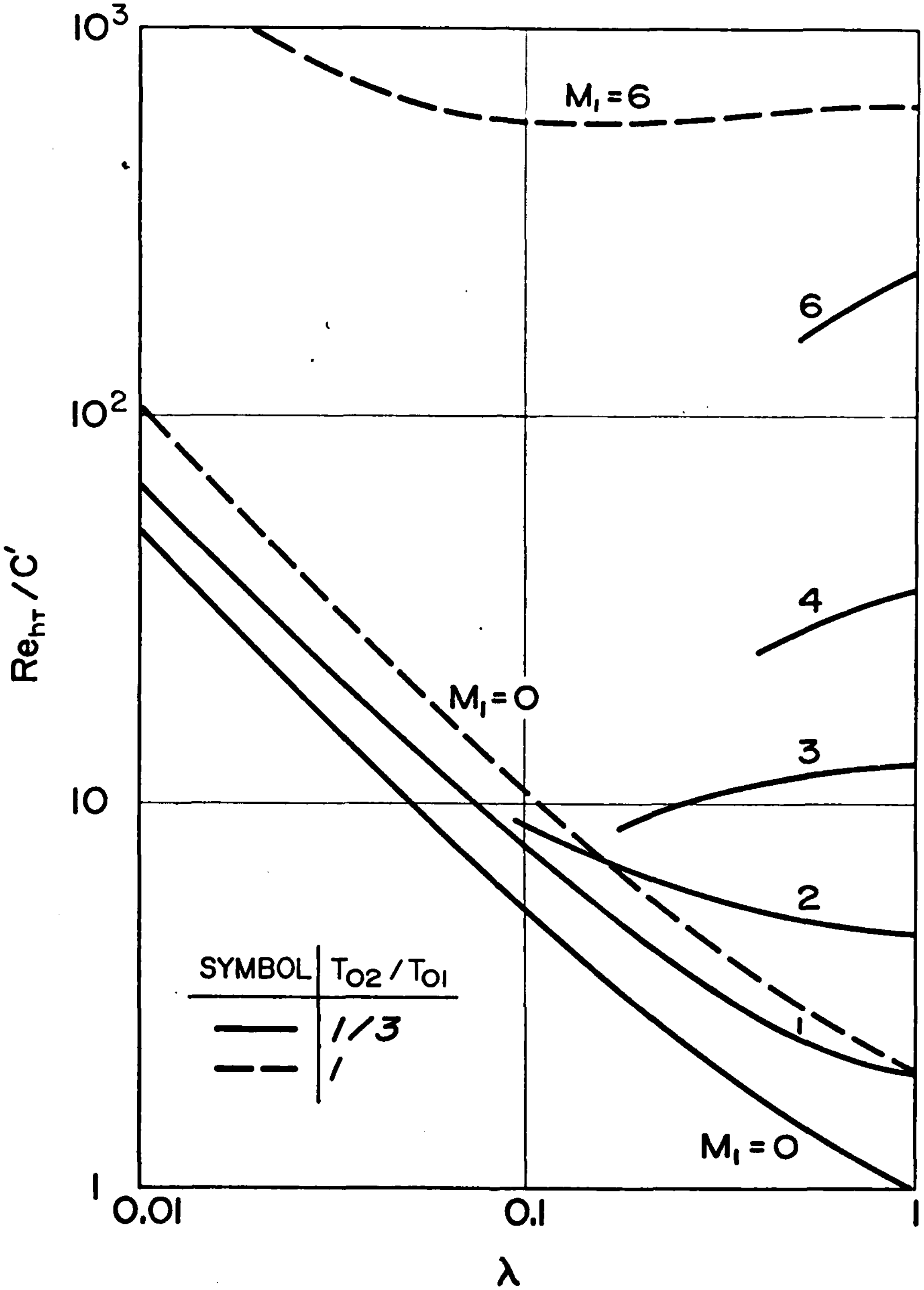

Figure 6. Details of the transition Reynolds number based on the FSL thickness, for the cooled case.

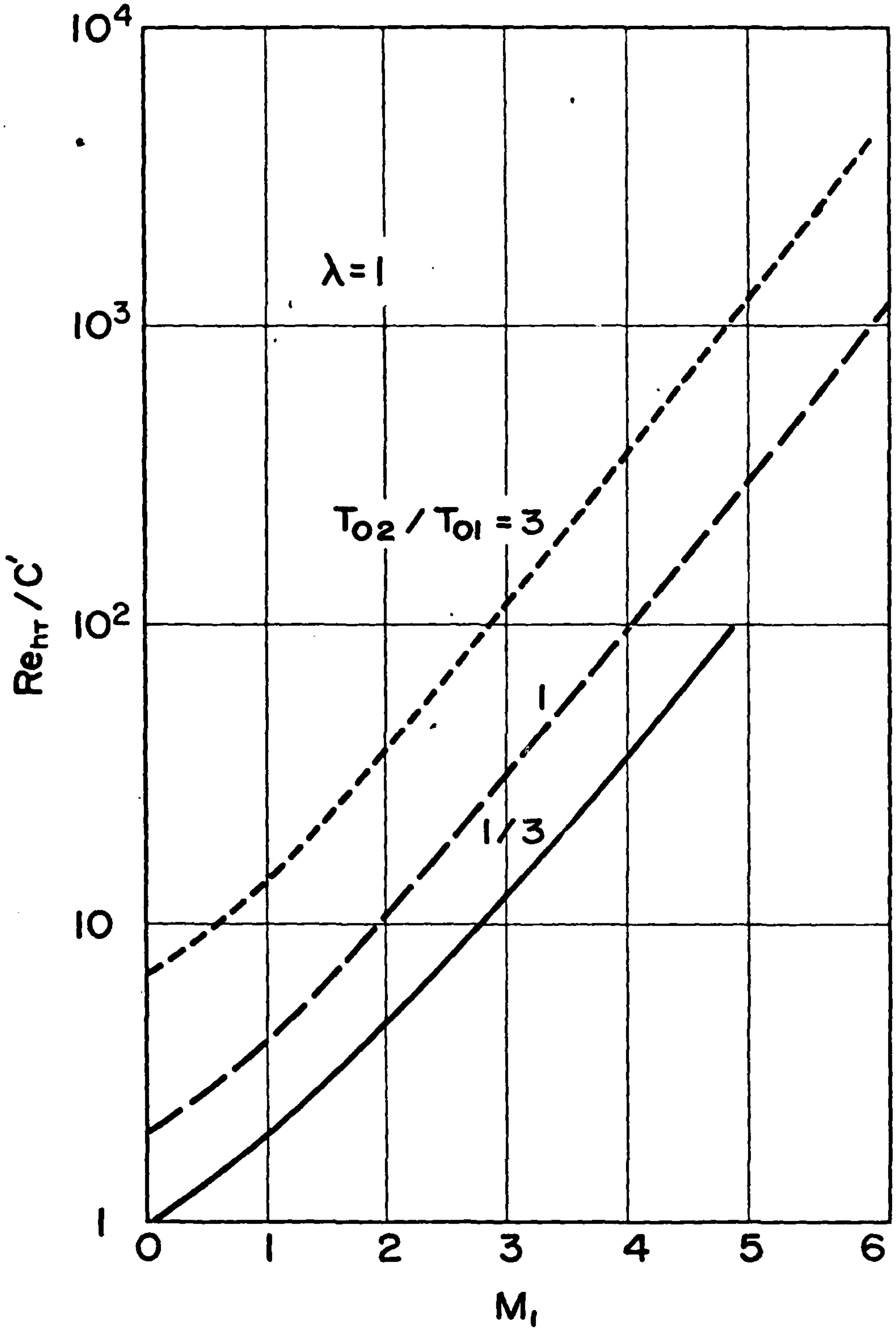

Figure 7. Transition of Reynolds number based on thickness, for the case where one side of the FSL is at zero velocity, showing the effect of heat transfer.

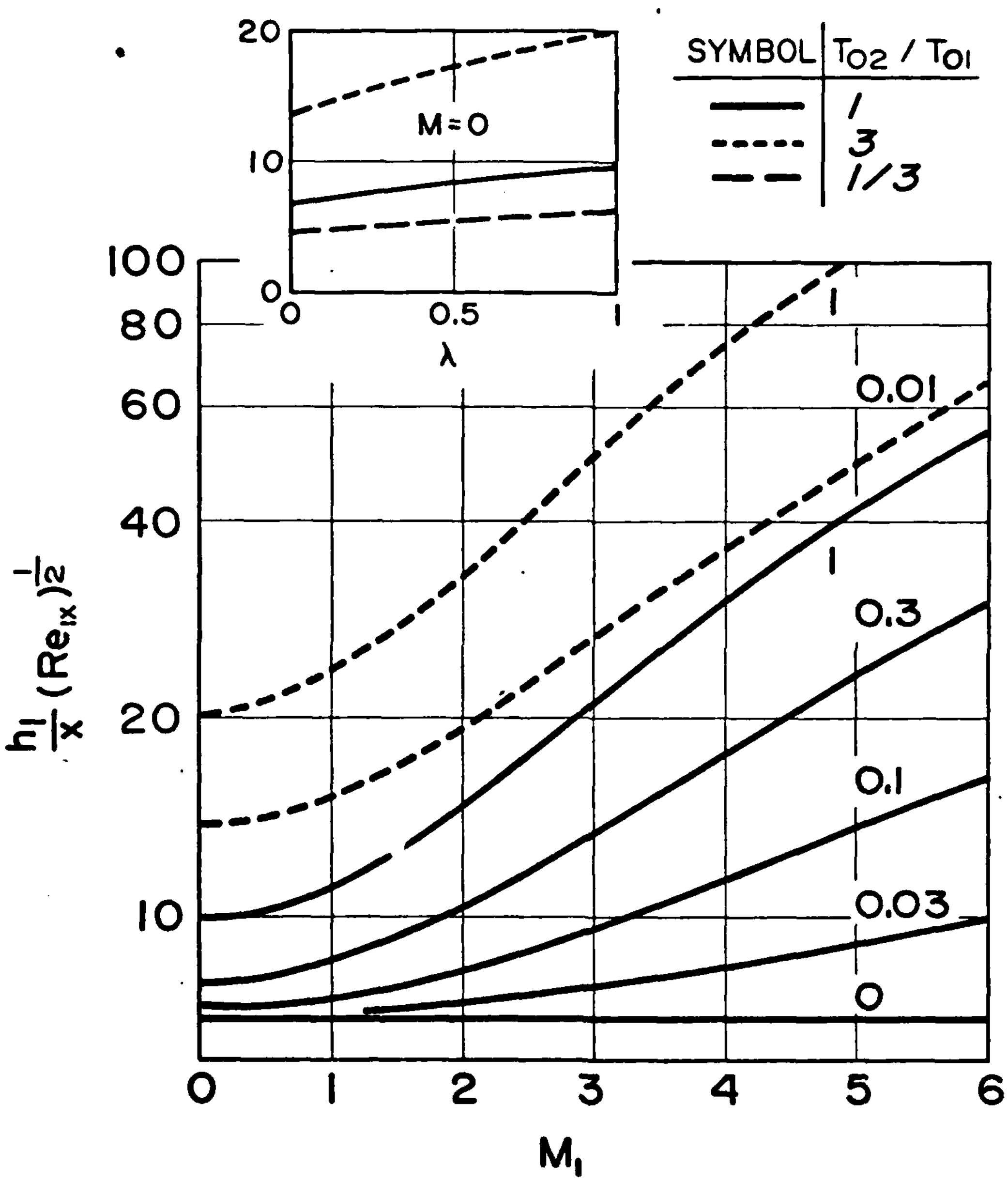

Figure 8. Laminar FSL thickness, primarily for the adiabatic and heated cases; the incompressible behavior is shown in the inset.

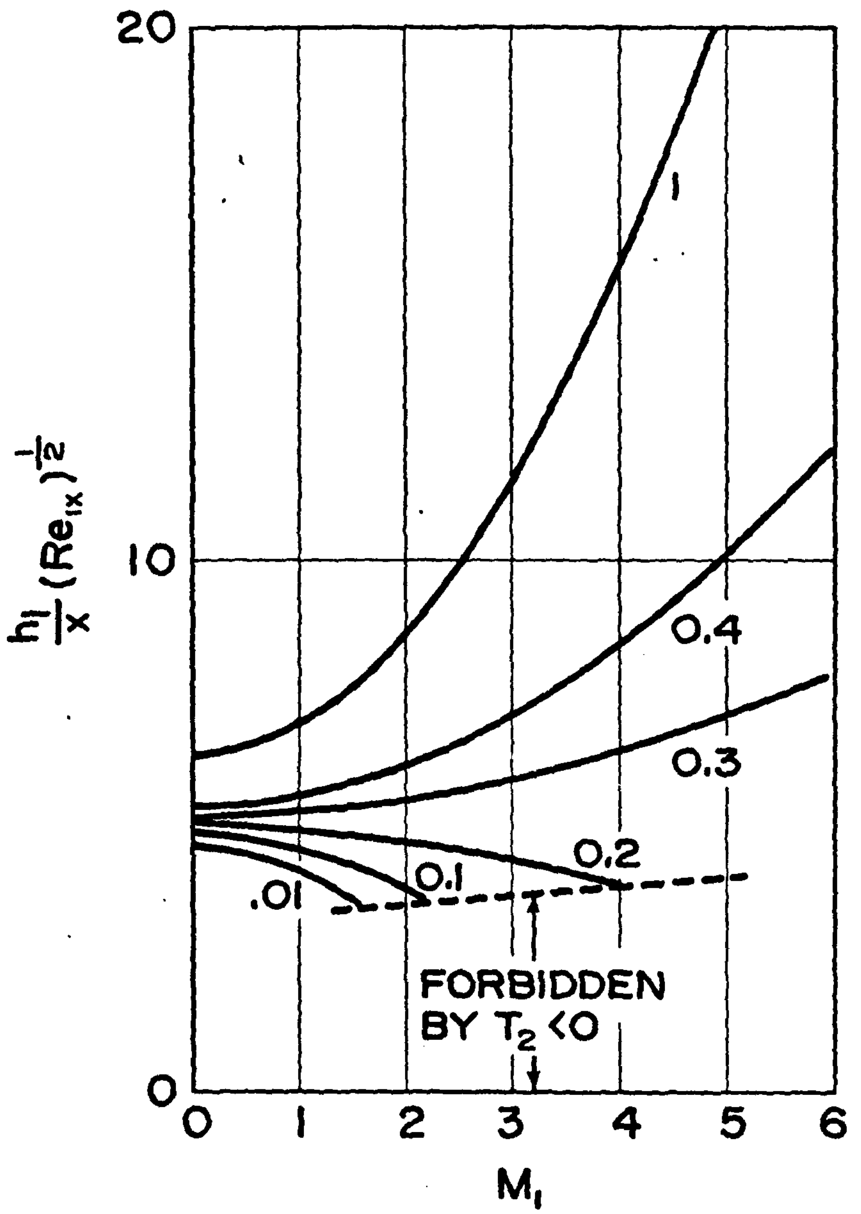

Figure 9. Laminar FSL thickness for the cooled case.

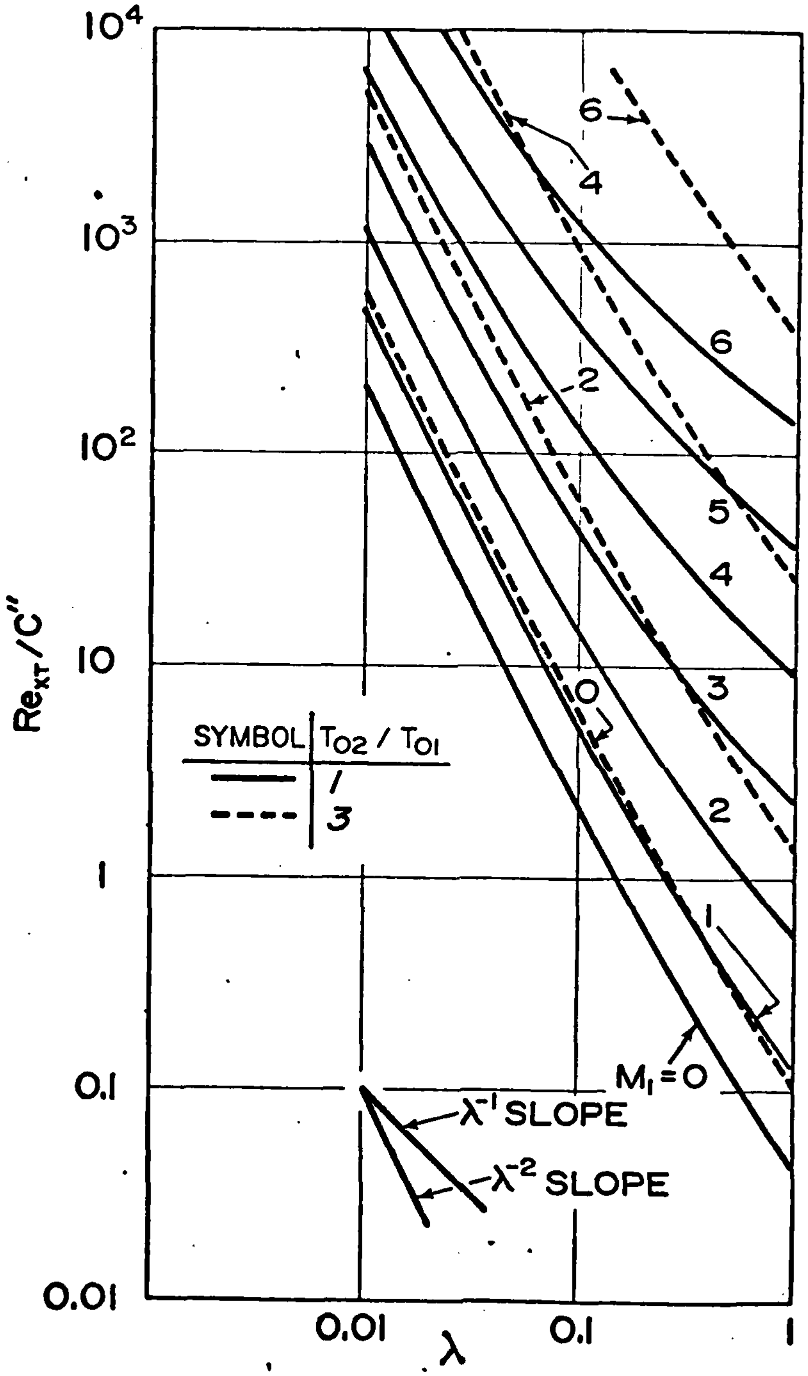

Figure 10. Transition Reynolds number based on distance from the actual flow origin: adiabatic and heated cases.

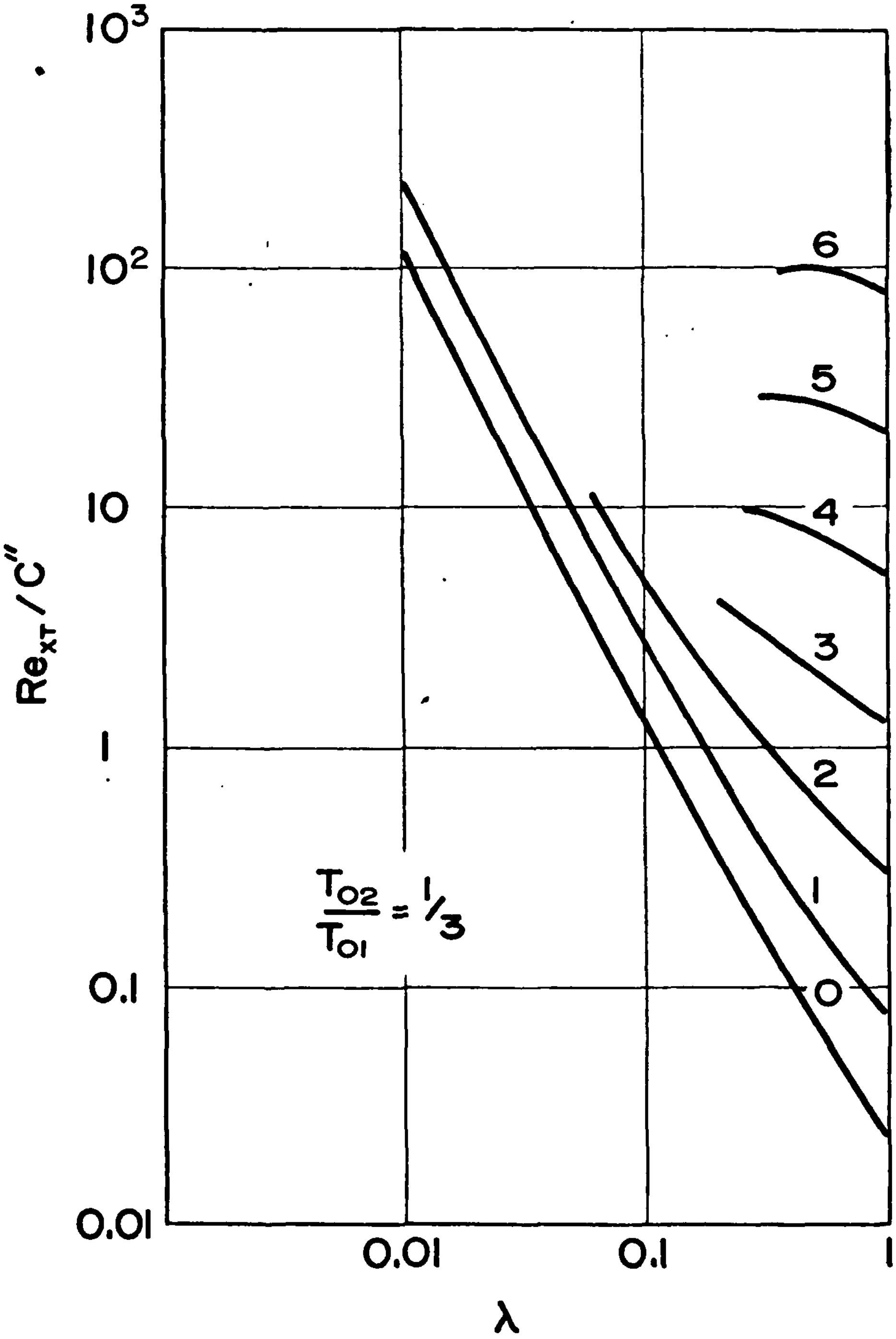

Figure 11. Transition Reynolds number based on distance from the actual flow origin: cooled case.

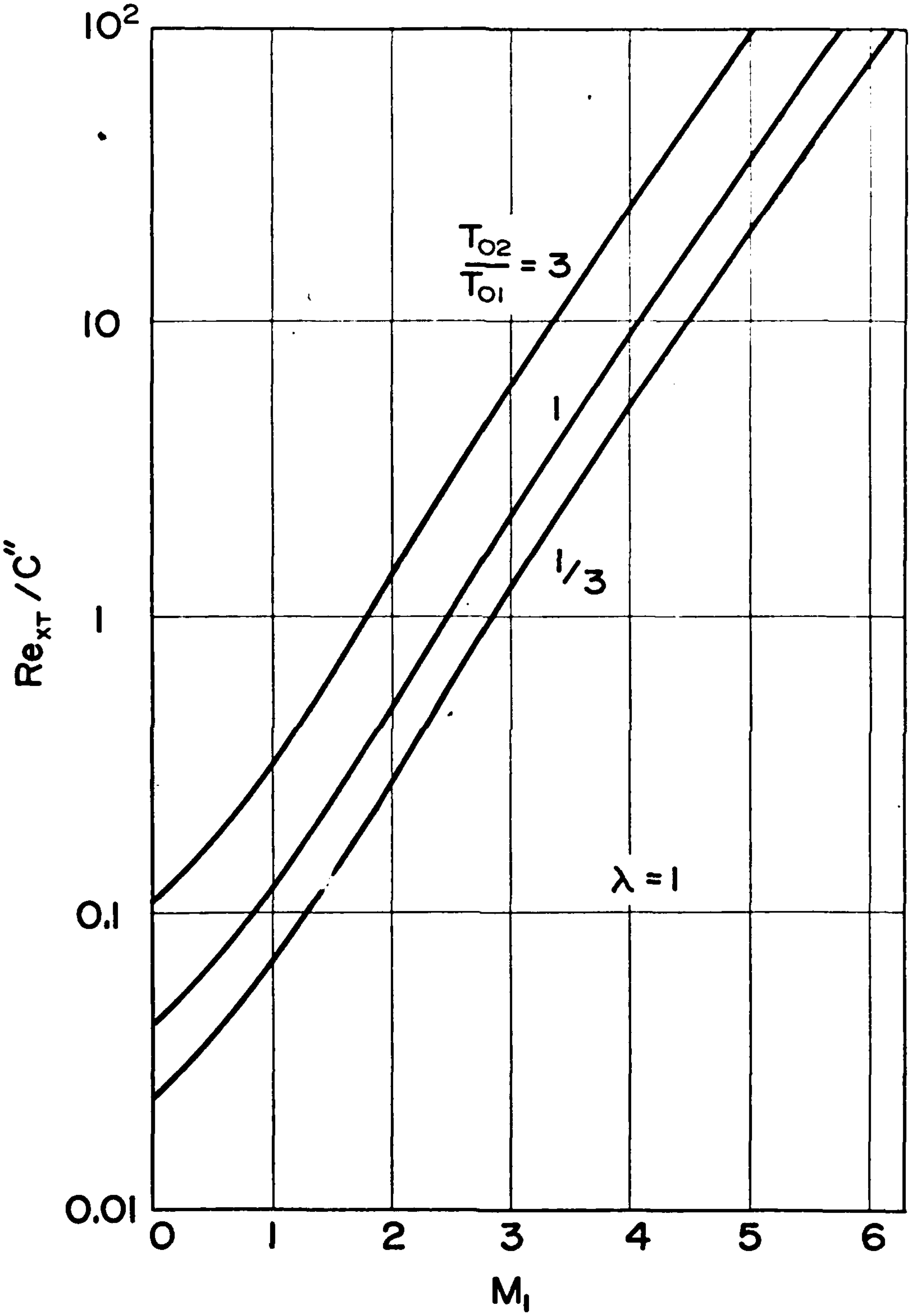

Figure 12. Transition Reynolds number cross-plotted for the case $\lambda = 1$ to show effect of heat transfer.

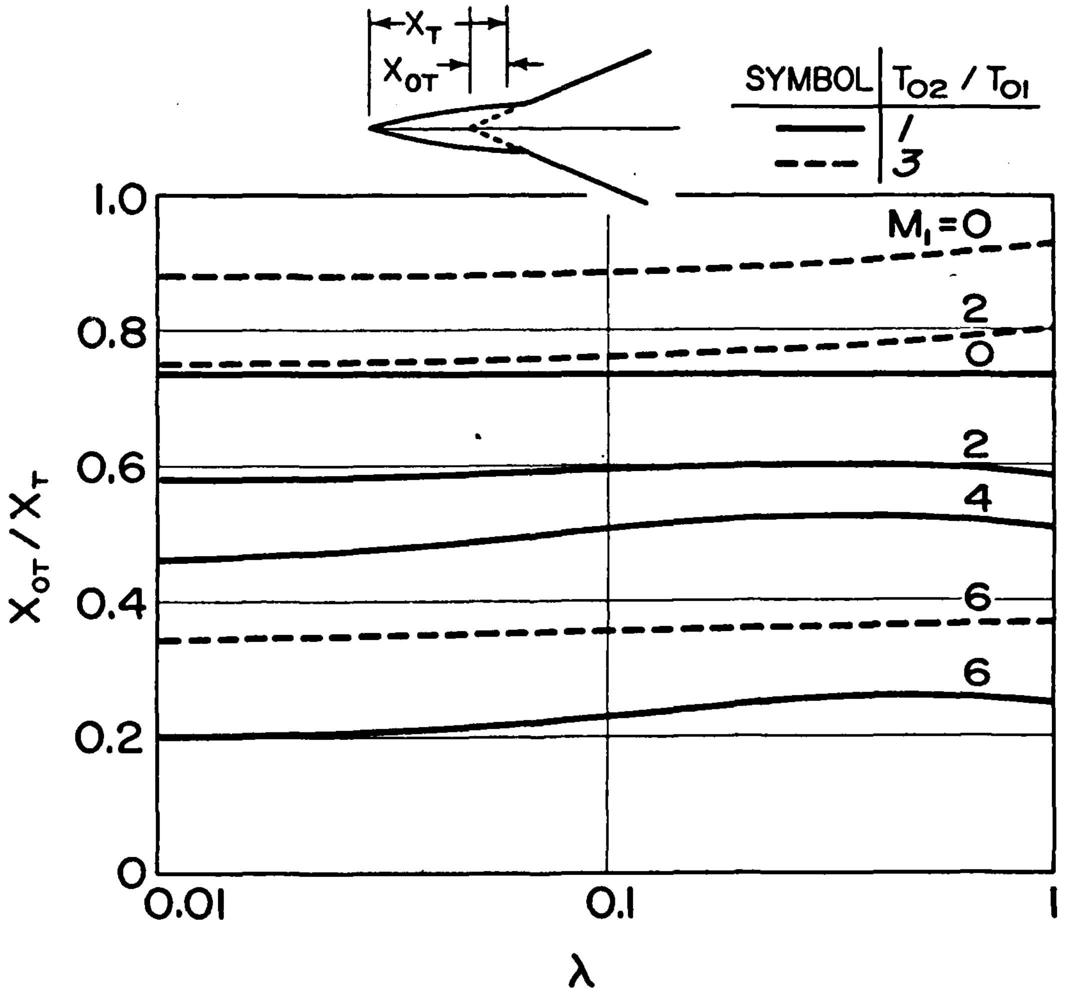

Figure 13. Relative position of the virtual origin of turbulence in a shear layer: adiabatic and heated cases.

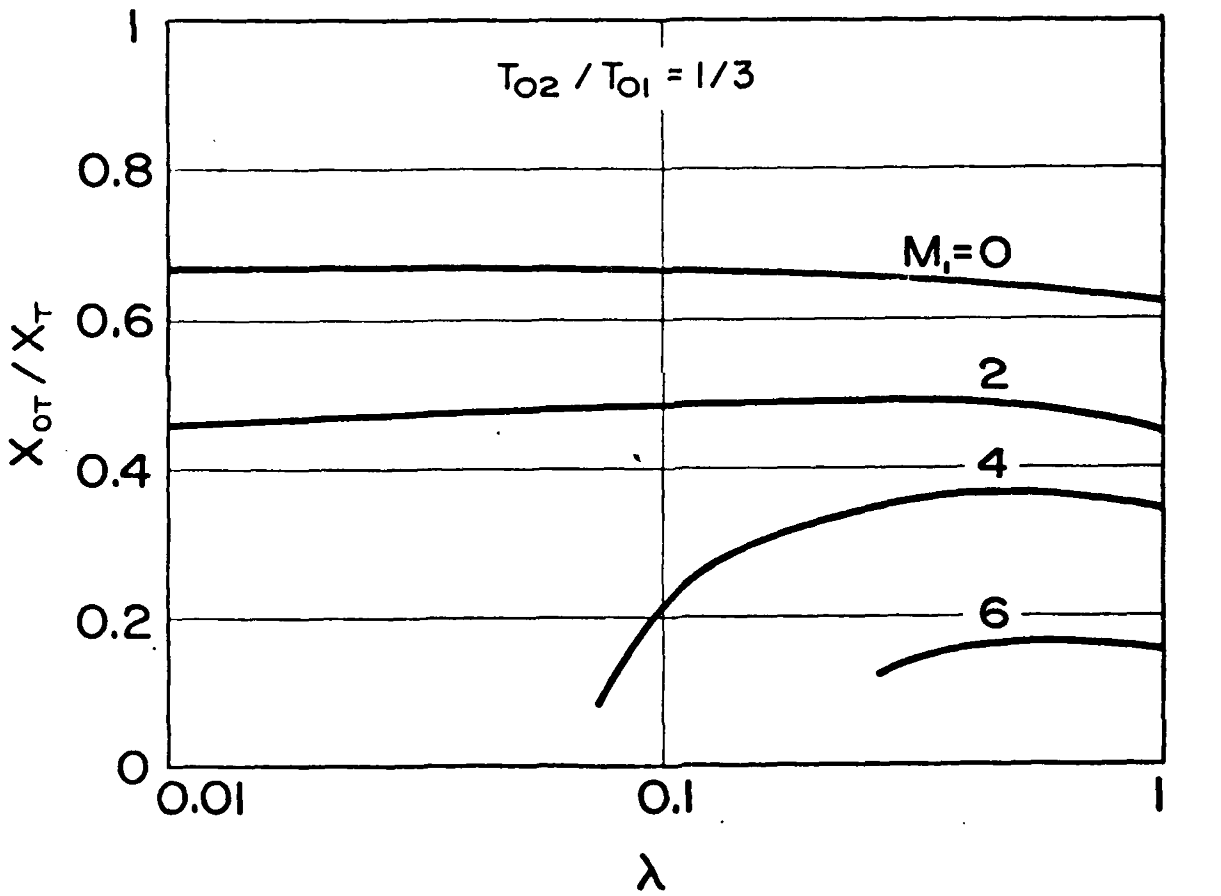

Figure 14. Relative position of the virtual origin of turbulence in a shear layer: cooled case.

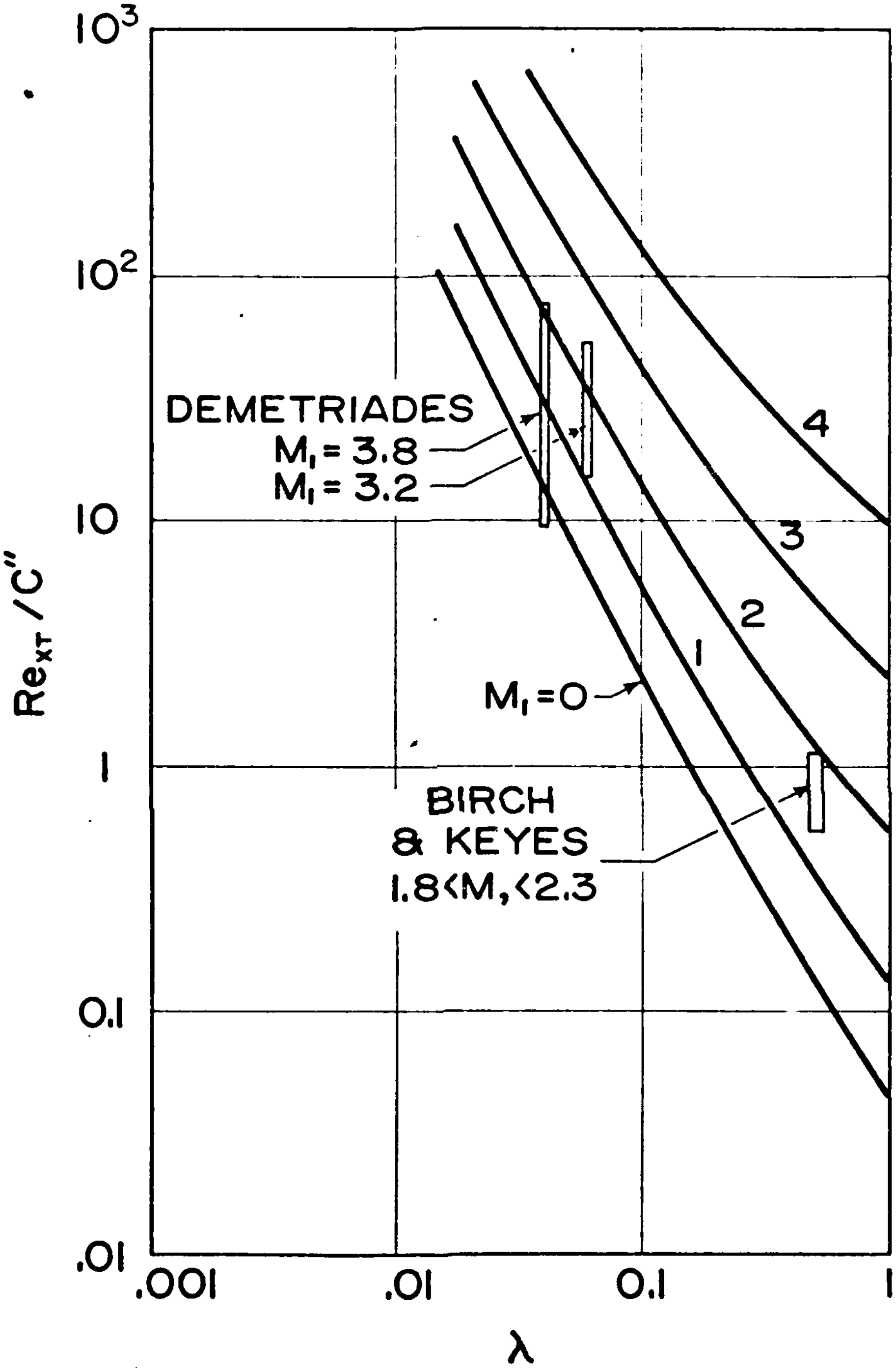

Table 15. Comparison of the present theory with experimental results, for the homogeneous adiabatic case (air).

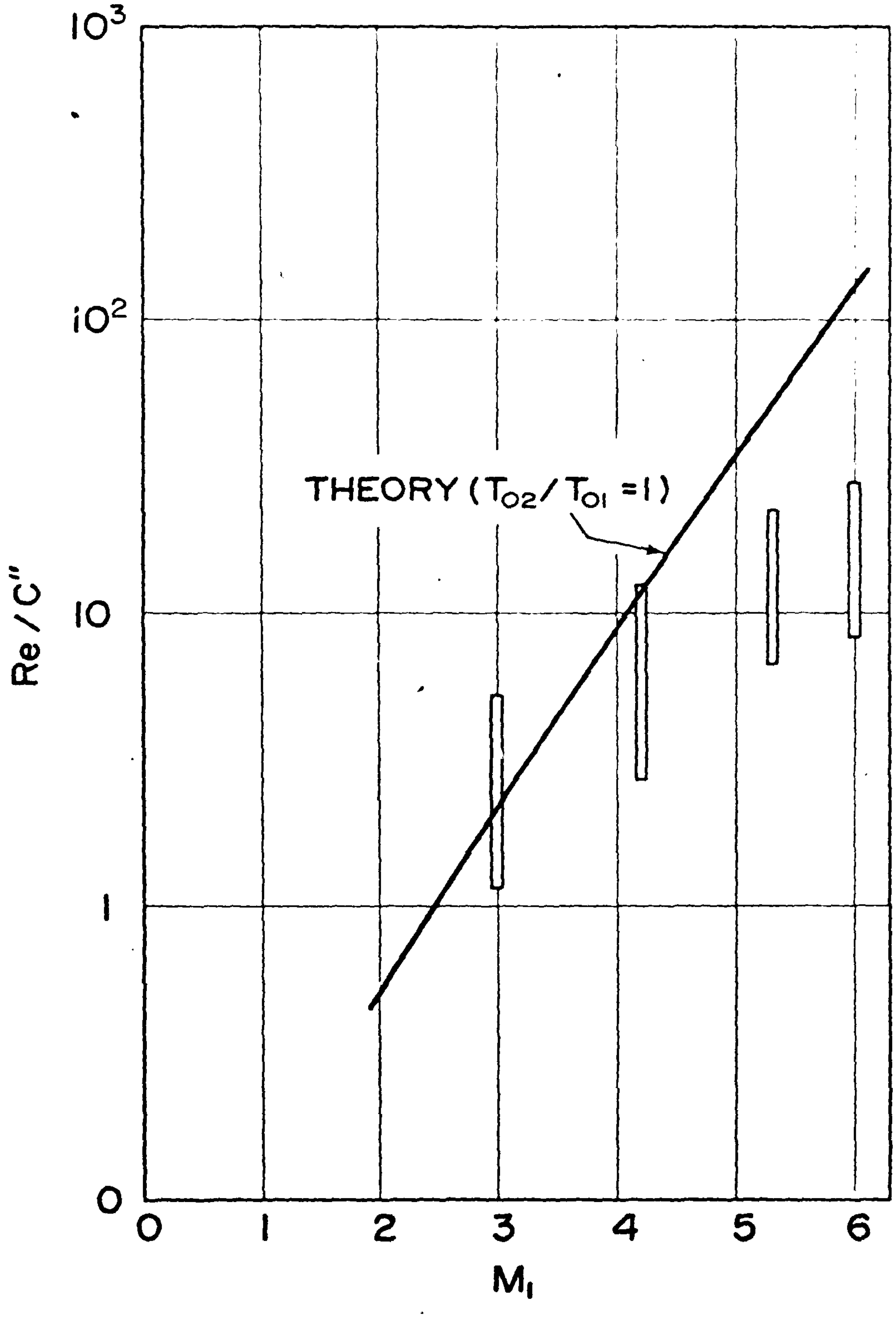

Table 16. Comparison of the present theory with experimental results, for the homogeneous adiabatic case (air).

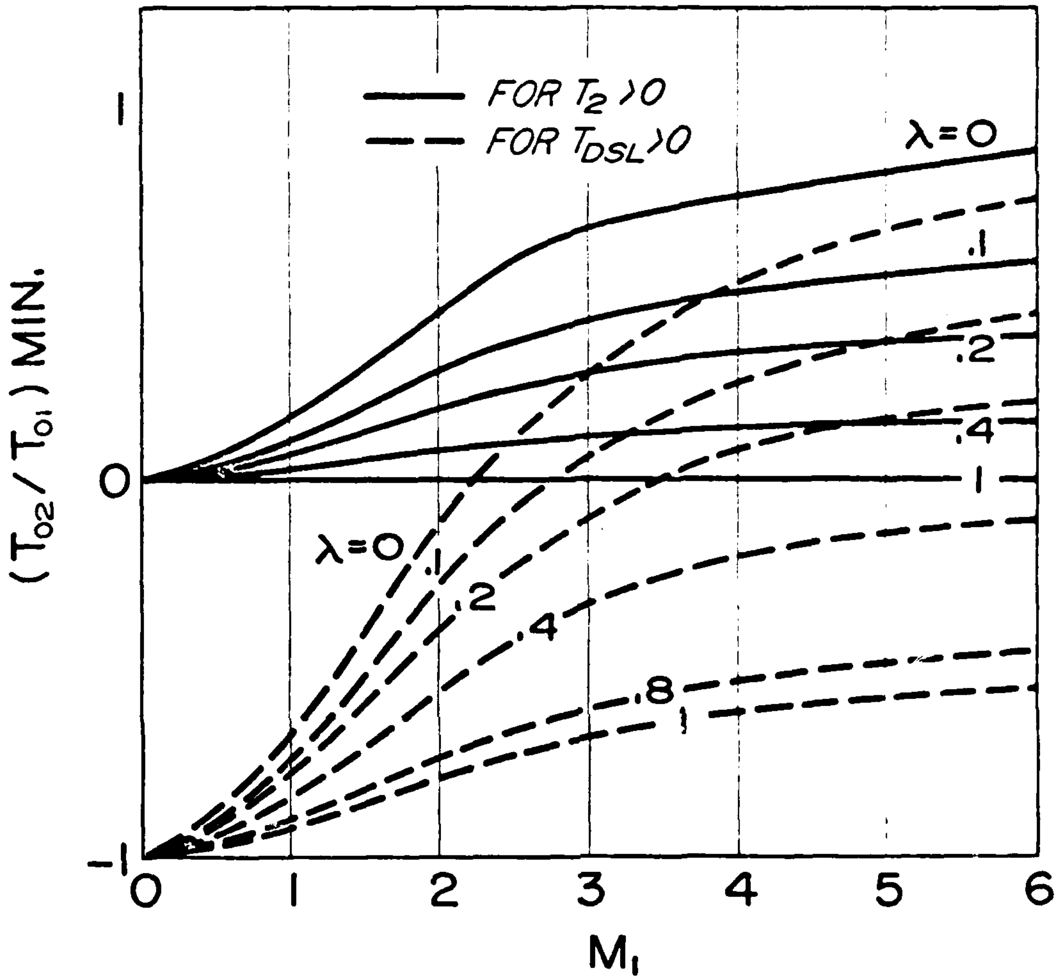

Table 17. Minimum permitted stagnation temperature for FSL flows if M_1 and λ are specified.

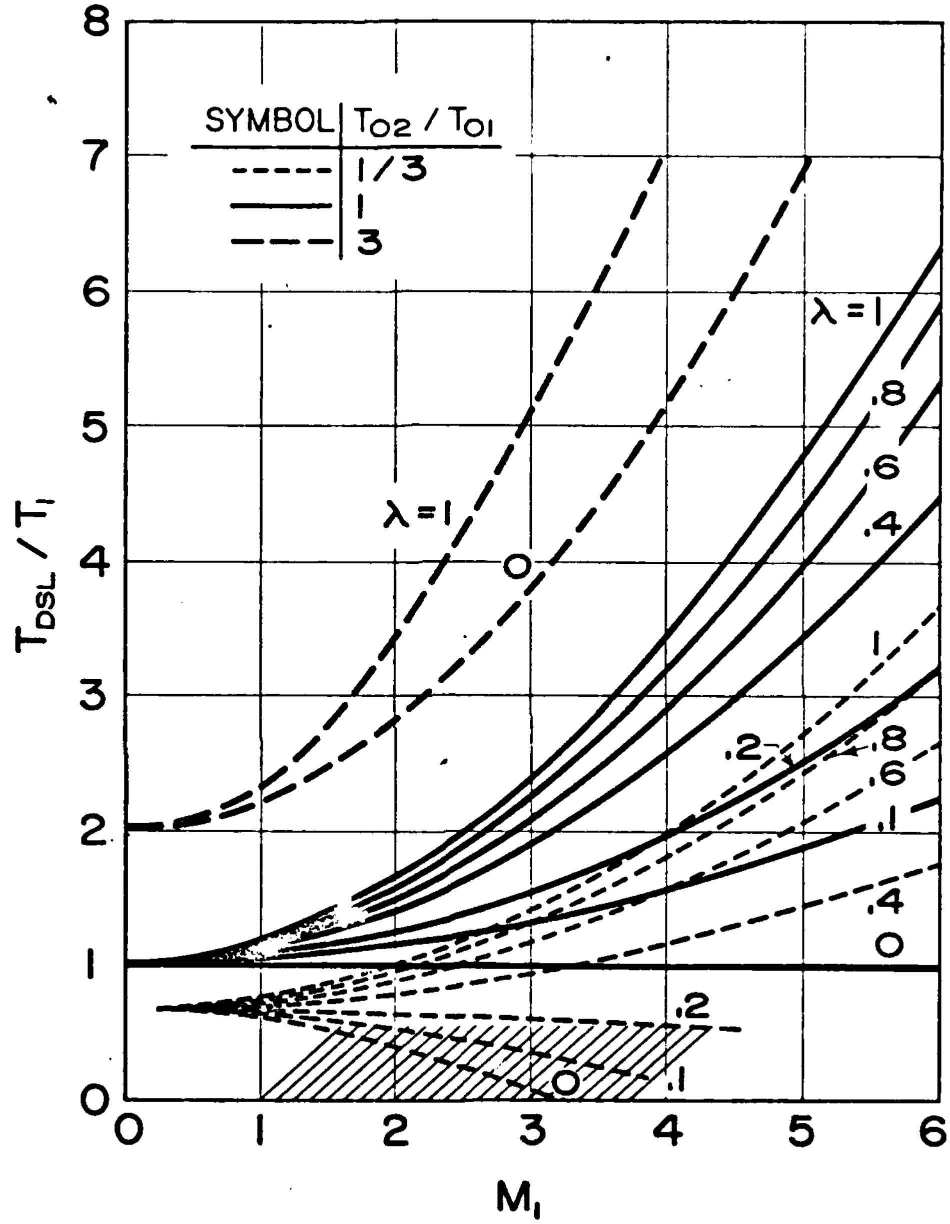

Figure. 18. Dividing streamline temperatures.